

Chapter 8. Atomic nuclear structures

Appendix: Atlas of atomic nuclear structures.

The Mendeleev's Periodical law and the pattern of the Periodical table are signatures of the nuclear building tendency of the stable elements (a conclusion apparent at the end of this chapter).

The technological achievements in different fields such as: biomolecular physics, nanotechnology, new materials, transmutation of elements (cold fusion) and so on indicate that the nuclear structure of the atoms is still unknown mystery. The Quantum mechanical models of the atoms, do not provide structural features of the atomic nuclei.

8.1 The Quantum Mechanical model of the atoms as a mathematical model only

The Bohr planetary model of the hydrogen atom despite its problems fits to the adopted by the Modern physics concept about the physical vacuum. The quantum mechanical models of the atoms are based on the Bohr planetary atomic model, but upgraded with with some additional rules. As a result number of workable models are defined for the atoms with additionally restriction rules and carefully selected parameters of the wavefunction solutions. Despite of this a pure theoretical model is quite difficult even for the Helium.

Let describing some specific features of the QM models of the atoms. Having in mind, that the number of the protons in the neutral atom is equal to the number of the electrons, the QM model uses the number of the electrons as an identifier and finds a rules for their arrangement in shells and subshells. The found rules are well suited to the element position in the periodic table. The use of the wave function with the proper set of quantum numbers successfully describes many spectral features as transition between different orbits. It is well known that the number of protons define the element and its chemical and physical properties. From the other hand the atomic spectrum that is the distinctive signature of any atom is related with the electron orbits.

The nuclear radius, according the QM model is in order of 10^{-15} m, while the size of the orbits is at least 10^4 times larger. Then a logical question arises: How the protons bundled in so small nucle-

us are able to define extremely well the position and shapes of all possible orbits? The QM mechanics is not able to provide logical (physical) answer of this question.

The strongest experimentally related arguments that QM uses for the planetary atomic models is from the scattering experiments. The Rutherford experiment is cited as a classical one, but many other experiments are also done. **One of the biggest confusion, however, comes from the fact that the output results from the scattering experiment rely on adopted scattering models, while the models themselves are strongly dependable on the adopted concept about the physical vacuum.** In order to obtain the nuclear size (or proton or neutron dimensions), for example, an interpretation scattering model is used. If considering the Rutherford experiment, the measured output result is the angular distribution of the scattering. The Atomic nuclear size is derived by admitting that it has a spherical shape. But a toroidal shape or a twisted torus with a proper thickness will provide the same angular distribution.

From the point of view of the BSM it appears that the obtained results may differ significantly from the reality because the following considerations are not taken into account:

- **the atomic nucleus is considered a spherical with a uniform density**
- **the structure of the physical vacuum is not taken into account**
- **the structure of the elementary particles involved in the scattering is not taken into account**

The above considerations indicate that for the case of the suggested concept about the physical vacuum all the scattering experiment should be reconsidered, because the real dimensions and shapes of the proton and neutron (and the atomic nuclei respectively) may appear quite different.

The QM models operate only by energy levels, so they do not give any information about the structural features of the atomic nuclei. In many cases they provide correct energy levels of the excited states or the energy interactions based on the discovered quantum mechanical rules and experimentally measured constants. While the QM rules are quite useful, the physical mechanism behind these rules, however, has been unknown so far. **Ac-**

According to the BSM, the QM models of the atoms are not real models but mathematical models only. In order to operate, the QM models need the uncertainty principle suggested by Heisenberg. This is dictated by the adopted concept about the physical vacuum (while the existing media is not apparent, the process of the photon emission and absorption has to be directly related to the position of the electron, but both processes are related with multiple electron orbital circling, so the uncertainty principle is necessary). In the suggested vacuum concept according to BSM, the photon emission is a result of the CL space pumping obtained by the multiple orbital circling of the electron. This opens a possibility for a classical analysis of QM phenomena without using of the Heisenberg uncertainty principle. Such new kind of analysis was shown in Chapter 7 for the hydrogen atom. Additional examples of such analysis are provided in Chapter 9 for estimation of vibrational energy levels of simple molecules (despite the shown methods give approximate value, they provide a valuable information about the proton and neutron configurations of the nuclei).

The QM models could not provide information about the real nuclear structure due to the missing following features:

- **the material structure of the CL space environment with its Zero Point Energy;**
- **the complex spatial structure of the atomic particles;**
- **the structure and the oscillation properties of the electron;**
- **the IG forces inside the Bohr surface;**
- **the distributed E-field of the proton inside the Bohr surface and the modified Coulomb law**

The IG field as seen from the total course of BSM is the most fundamental physical law behind the known fields (Newtonian gravitation, electrical and magnetic). It is directly involved in the nuclear binding energy and is apparent in the vibrational properties of the atoms in the molecule (as shown in Chapter 9). However, it is completely hidden in the QM models of the atoms.

8.2 BSM concept about the atomic structure

According to BSM, the proton has a shape of Hippoped curve with a parameter $a = \sqrt{3}$ and a length of 0.667×10^{-10} m. The proton core thickness is 7.84×10^{-13} m, while its cut length is 1.627×10^{-10} m. The proton is only a twisted shape of the proton-neutron - a primary stable particle as a result the particle crystallization process, which has preceded the birth of the galaxy (as discussed in Chapter 12). The proton-neutron shape is a torus, but this shape is not stable in CL space. The proton and neutron contain same types of helical structures (torus and curled toruses), the difference between them is only in their overall shape. All the FOHSs have internal RL lattices that are able to modulate the CL nodes of the surrounded space by their IG field. In the shape of the neutron, the external modulation from the RL IG field appears symmetrical and forms a proximity field that is locked by the IG field. In the shape of the proton the external modulation from the RL IG field is not symmetrical, so it appears unlocked and created a positive charge as a spatial domain of positive EQs. In both cases the charge in the proximity is distributed around the external shell. This feature provides the conditions of the quantum orbits. Therefore the orbital traces of the electrons are strictly defined by the proximity E-field.

The electron is a single coil helical structure whose external diameter is very slightly larger than the proton thickness $2(R_c + r_e) = 7.9 \times 10^{-13}$ m.

The BSM theory was able to unveil the atomic structure of all elements as an spatially ordered systems, composed of the basic particles proton and neutron. The mutual spatial positions of the protons and neutrons in the atomic nucleus is one of the most important atomic feature for every element. Their arrangement is defined by the shape of the proton and neutron, the IG fields and the distributed E-field around the proton core, inside the Bohr surface (see the definition of the Bohr surface in Chapter 7). Such nuclear structure defines separate orbital quasiplanes for every proton. The electrons are subordinated to occupy the orbital quasiplanes inside the Bohr surface of the protons. The individual Bohr surfaces from closely connected protons may combine in one integrated Bohr

surface. The electron orbits of the neutral atom are always inside the integrated Bohr surface.

8.3 Atlas of atomic nuclear structures

The nuclear configuration for the most abundant isotopes are shown in an appendix titled: Atlas of Atomic Nuclear Structures (ANS). In order to simplify the drawings of the complex three dimensional nuclear shapes, two dimensional sketches are used where the basic elements (protons and neutrons) are shown by corresponding graphical symbols. Figure 8.1 shows these symbols and their use for a graphical presentation of some of the most simple elements: hydrogen deuterium, tritium and helium.

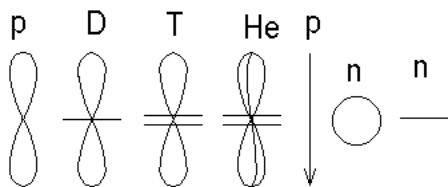


Fig. 8.1

Symbols for atomic nuclear structures

The following notations are used:

p - Proton
 D - Deuterium
 T - Tritium
 He - helium
 n - neutron

8.3.1 Building rules of the atomic nuclei, related with Z number

Using the Z number as an argument, the build-up trend is investigated and the following rules are discovered. They are logical consequences of build-up process, governed entirely the natural forces (see §8.3.2).

- **Chain building principle: a consecutive building of complex structures by starting from simple basic one and bonding additional basic structures**
- **End product of particular element: a compact shell structure formed of basic elements arranged according to natural rules and kept stable by the close proximity IG field (and electrical field) in CL space environments**

- **Natural selection of the stable atomic structures: a process relying on the radioactive decay**

8.3.2 Natural forces involved in the atomic build up process:

- **External gravitational pressure**
- **Proton - proton repulsion**
- **Neutron - proton near field interaction in the moment of neutron insertion over the proton saddle**
- **IG (Intrinsic gravitational) attraction between protons and neutrons**
- **Dynamical interaction between the internal RL(T) of the protons and neutrons and the surrounding CL space**
- **Space locking of the proton electrical field by the orbiting electron and the IG field (for a neutral atom only)**

8.3.4 Complying to discovered naturally existing rules and principles

- **Periodicity in the atomic structures corresponding to the periodical table**
- **Complying to chemical valencies**
- **Complying to Hund's rule**

8.3.5 Useful data for unveiling the nuclear structure

- **X-ray properties of the elements in a solid state.**
- **Laue back-reflection patterns**
- **Relation between the nuclear bonding energy and the X ray spectra of the elements**
- **Oxidation number by experimental results. Principal and secondary valencies.**
- **Ionization potential dependence of Z number**
- **Considerations for orbital interactions and pairing between the electrons from different orbitals**
- **Radioactive decay of unstable isotopes**
- **Optical atomic spectra**
- **Photoelectron spectra of molecules**
- **Nuclear magnetic resonance of the elements**
- **Nuclear configuration and VSEPR model for chemical compounds**

- **Vibrational properties of the atoms in the molecules in a gas phase.**

8.3.6 Type of bonds in the atomic nuclear structure

The protons and neutrons in the nuclear configuration are kept together by different types of bonds. The abbreviated notations of these bonds are given in Table 8.1.

Bonds in the atomic nuclear structure
Table 8.1

Bond notation	Description
GB	Gravitational bond by IG forces
GBpa	polar attached GB
GBpc	polar clamped GB
GBclp	(proton) club proximity GB
GBnp	neutron to proton GB
EB	electron bond (weak bond)

8.3.7 Basic rules in the process, leading to build-up of stable isotopes.

The build-up process of the structures shown in Fig. 8.1 is quite evident. However, it still requires special external conditions. To be inserted over the proton, the folded neutron has to overcome initially the repulsion forces between its proximity near E-filed (locked by the IG field) and the proton E-field. The build-up of He from two Deuterons, also requires special environments. It causes, also, a large amount of CL space energy to be freed as a result of a CL space shrinkage (bonding energy). The He atom possesses largest IG field density in comparison to other basic structure. So it is quite reasonable to be embedded as a He nucleus in the nucleus of any stable element. The shape of other basic components allow them to be attached to the He nucleus. Following this logic, and the considerations in §8.3.4 and 8.3.5, it is discovered that the trend of congregation into larger atomic nuclei leads initially to building of polar structure, in which the He nucleus is in the middle. After such structure is completed to some level, at which the equatorial radius is larger than the polar one, the build-up trend leads to connection of such struc-

tures in the polar regions. As a result of this, the build-up trend leads to a polar-connected chain structure. After the building of three polar connected structure, the build-up trend changes to mostly equatorial growing, in order to approach more spherical shape. The envelope of the completed polar structures and their interconnection are illustrated in Fig. 8.2.

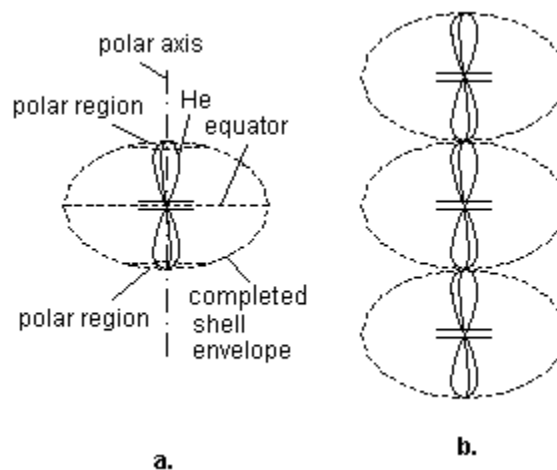


Fig. 8.2

a. - polar structure; b. - polar-chain structure

The detailed analysis of the build-up trend leads to discovering the following rules:

- (1) The build-up trend, following the increase of Z number, leads to a building of congregation of polar-chain structure. The first level of the congregation is a completed polar structure containing He in the centre. The second level of the congregation is a chain connection of completed polar structures in the polar region. This trend appears valid up to three polar structures (see Fig.8.2.b). The third level of the congregation is related with build-up process in which basic components are attached in equatorial regions. In such case the atomic nucleus approaches a more spherical shape. The first level of the congregation is completed at Ar. The build-up phases for the second and the third levels overlap. The third level of the congregation is a build-up of equatorial shells, so the nuclear shape tends to approach a more spherical form.
- (2) The building of the atomic nuclei is based on a process of bonding of basic elements (proton, Deuteron, Tritium, Helium). Once bonded, every basic element is kept in that position **due to the IG fields involved in the synchronization between the in-**

ternal RL(T) of all involved FOHSs. Such type of synchronization efficiently eliminate the repulsive forces between the separate protons.

This type of bonding is named gravitational (G. bonding). Four different types of G. bonding are distinguished: GBpa, GBpc, GBclp, GBnp (see Table 8.1).

(3) The main bonding mechanism, responsible for the atomic build-up is the polar gravitational bonding. It appears in two types: - polar attached GBpa, and polar clamped, GBcp

(4) Every GBpa bonded proton (Deuteron or Tritii) has some rotational freedom of motion in the polar plane, but very limited freedom in the equatorial plane. Neglecting the equatorial freedom, the proton position may be defined by the angle between the nuclear polar axis and the the long axis of the proton.

(5) Polar region problem: The polar electron circles around the core of all Gpa bonded protons (Deuterons or Tritii). This is a place of increased IG field density and concentrated E-field lines. The protons contributes to this IG field concentration, while the neutrons over the proton saddle, pull up the field to the periphery. For the stable isotopes a correct balance between proton and neutron number exists. Unstable isotopes converts to more stable elements by β^- or β^+ radioactive decay.

(6) The Hund's rule exhibits four type of appearance: two types of orbital pairing and two types of QM spin pairing. The different types of pairing possess different **pairing strengths**.

(7) The proton shell build-up trend matches the corresponding row of the periodic table. The isotope is stable, if the spatial arrangement of the protons fulfils the Hund's rule according to which the largest possible pairing strength appears as a dominant.

8) For Z- numbers larger than 23 or 28 more that one branch of the growing trend are possible. Some branches may pass through a zone of unstable isotopes and reach a stable isotope zone again.

9) The single polar structure is completed at Argon atom. The additional nuclear growing by bondings in the both polar regions continues to the group 10 (of periodic table), where it is interrupted. The probable reason is the balance between the gravitational field and EM field of external protons. Group 11 is from another branch that has been grown in

one pole only, but has been unstable. From groups 11 to 18 this branch is stable and the growing trend is completed at the noble gases.

(10) The growing mechanism for the atoms after Argon, could be based not only on a bonding of basic structures but also on an attachment of smaller nuclear structures, either with completed or not completed shells. The attachment is also at the polar region, but conditions for a clamp type of bonding are required (GBpc). This may reduce the probability of such growing.

(11) The external atomic structure that determines the chemical valence have similarity for the groups between 11 and 18 up to the element Rn. The Lantanides and Actinides have different external structures, not matching the structures of the mentioned above groups.

(12) For the groups 11 to 17 another weak bonding mechanism, named electron bonding (EM), interfere the main build-up mechanism, based on a polar bonding. It is based on interaction between quantum orbitals and is related with the Hund's rule. The EB bonded protons are excluded from the chemical bonds. Under influence of a strong chemical reagent, however, they could be unbonded.

(13) The weak EB bondings converts to strong GBclp bondings at group 18. In such case, the protons could not participate in any chemical bondings.

(14) A chain of three polar structure is completed at Xe atom and the additional chain growing is intercepted. Then a tendency to equatorial growing predominates, leading to build-up of the Lantanides (In the periodic table the Lantanides are shown after Ba, but the position of the two polar protons in Ba are preserved in all Lantanides).

(15) The Lantanides grow by GBclp bonding of deuterons (proton, tritii) to the equators of the two ends polar structures. They periodically become EB bonded in pairs due to orbital pairing (Hund's rule). Their EB bondings behave differently due to the different spatial positions of the protons. Such bonded protons (D,T) become underlying shells in the next following elements, but they can not be converted to strong GB bondings. They are source of alpha particles in the alpha radioactive decay.

(16) The nuclear structures from Hf to Rn grow by GBcpr bonding of deuterons (tritii) to the equators of the middle and two end polar structures, forming

two shells (2 x 8) with a rotational helical symmetry.

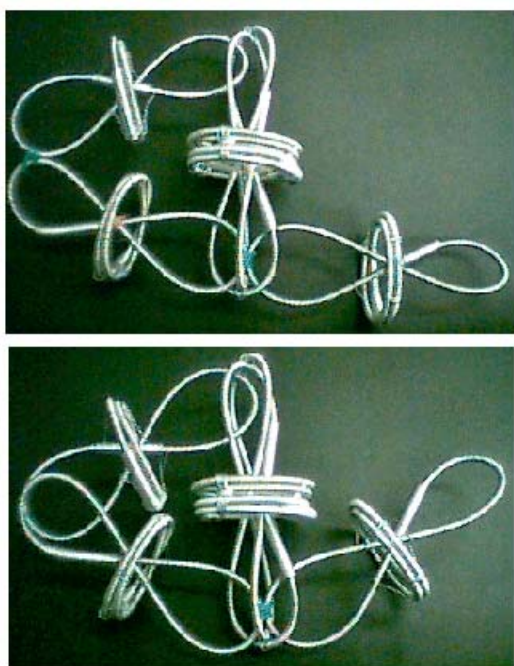
(17) The Actinides grow by GBclp bonding of mainly tritium (proton, deuteron), to the equators, forming another two shells between these of Hf - Rn.

(18) All atomic nuclei exhibits a higher order helicity possessing the same handedness as the proton.

Additional less general features will be discussed in the next paragraph.

8.3.8 Discussion about the basic rules

Fig. 8.3 shows mechanical mock-ups for illustration of the building process.



a.
b.
Fig. 8.3

Fig. 8.3
Illustration of spatial aggregation by bonding of basic structures

Polar angle of the polar bonded proton and its range of freedom

The central structure to which Deuterons are bonded by GBpa is a He atom. This GBpa bonding allows a freedom of rotational motion in limited angle (about 90 deg) in the polar plane as illustrated in Fig. 8.3. The freedom of motion in a plane parallel to the equator is only a few degrees. It is evident that the freedom of motion is restricted by the

hardware structure and the E-field inside the Bohr surface. The electrical interaction, for example, will not allow the free ends of protons to be so close as shown in case **a**. In one case of Hund's pairing the free ends could approach the case shown in **a**., but little bit apart, in order to have a room for both circling electrons to pass between the proton clubs. In case **b** a BGclp type bond is shown. This type of bond exists in the internal proton shells and in the external shell of the inert gases.

Neglecting the equatorial freedom, **the position of the proton could be defined by the angle between nuclear polar axis and the long axis of the bonded proton**. This angle may be defined as a **polar angle**, characterised by an angular range and boundary conditions.

- **The polar angle approaches zero (but could not reach), when the free proton club is far from the equatorial plane.**
- **The range of the polar angle is restricted from the structural configuration and pairing with protons, bonded in the opposite pole of the nucleus.**

The polar angle and its range are very characteristic parameters of the valence proton. The ranges of the polar angles of the protons are different in the different elements.

The four types of the gravitational bonds and one type of the electron bond are shown in Fig. 8.4

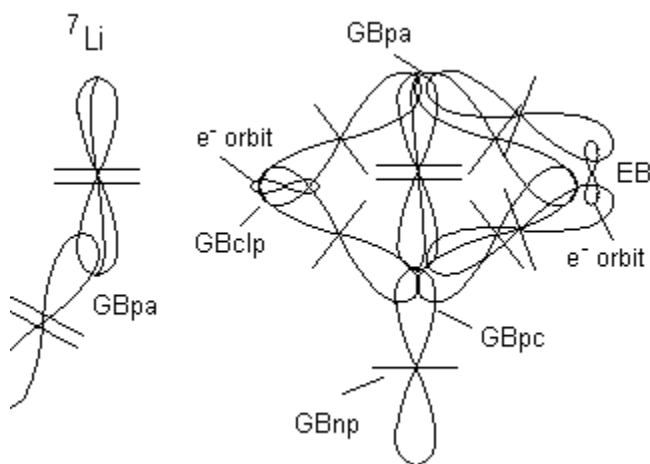


Fig. 8.4

The left structure is ${}^7\text{Li}$ nucleus, while the right structure is a portion of nucleus. The annotation of the different type bondings is according to Table 8.1

The electron bond (EB) corresponds to one type of Hund's rule electron pairing. The common electron orbits for EB and GBclp bonds are also shown. The electron orbital plane for EB is close to the polar plane of the atom, while the electron orbital plane of GBclp is close to the equatorial plane of the atom.

It is evident from Fig. 8.4 that when using the Hippoped curve symbols, the drawing become very complicated for elements with high Z number. For this reason, in the Atomic Atlas drawings, only the He symbol is used in the centre, while the protons are shown as a vectors (like symbols). Even in this way the drawings of the heavier atoms become overcrowded. In such case, an additional drawing simplification are used as the following:

- more complex nuclear structures are shown by three views (projections) ; the middle projection is a polar section; the top and bottom are polar views.

- the polar view shows the peripheral structures from its side only and without showing the helicity

- in the polar view, the angles between the symbolic vectors, and the vectors lengths may deviate from the real perspective view, for reason of drawing clarity

- completed and known internal structure (like Ar), when participating in element with higher Z number, may be shown by dashed shaped oval or polygon (close to the structure envelope)

- the nuclear helicity is not shown in the drawings

- additional symbols for electron bonding (EB), corresponding to Hund's rule are also used.

Electron pairing and Hund's rule.

In §7.11 the magnetic field related to the electron magnetic radius was discussed for the single proton. It was emphasized, that it is kept inside the Bohr surface. When more than one protons are connected to the polar region of the He nucleus, their individual Bohr surfaces become connected into one **integrated Bohr surface**. This surface now closes a common volume. In such case, it is possible the magnetic fields, related to the magnetic radii of the electrons to interfere. The electrons are still in their orbits, but their QM spins become mu-

tual dependent. This affects the position and orientation of the orbits of the different protons and consequently the proton position (having in mind, that the proton has some angular freedom in the polar nuclear plane.)

There are number of differences between the QM model and BSM model that reflects also to the terminology:

(a) the electrons in QM model circulate around a common nucleus, containing all protons and neutrons

(b) the electrons in BSM model are strongly connected to their protons

One or more electrons according to BSM may pass to other protons only in special cases like: an Auger effect; a radioactivity decay, a mutual alignment of valence protons, bonded to one pole.

(c) According to QM model, the atomic element position in the Periodic table is directly related to the electron orbits, defined by shells and subshells

(d) The electronic shell and subshell configurations, used in QM model, do not have the same physical arrangements in the BSM model, but the ionization energies are the same.

(e) The orbital quasiplanes for the valence protons in the atoms are of similar type as the orbitals in the Hydrogen, corresponding to its spectral series: Lyman, Balmer, Paschen, Bracket etc. The Lyman series, however, is significantly restricted for heavier atoms, while the Balmer one is always available. The restriction of the Lyman series depends also of the aggregated state.

Despite the above differences, the BSM model provides excellent match of the atomic elements to the periodic table with clearly defined building rules. The BSM model provides also clear physical explanation of the Pauli exclusion principle and the Hund's rule. The Pauli exclusion principle, discussed in §7.11 for the Hydrogen atom is valid in a similar way for all atoms.

The Hund's rule according to BSM model appears in two options, each one possessing two sub-options:

- orbital pairing
- electron pairing

The orbital pairing subdivides additionally into:

- orbital pairing for protons attached to a common pole
- orbital pairing for protons, attached to different poles

The electron pairing also is valid for two cases of the proton bondings: EB and GBclp.

The different options of the Hund's rule are illustrated by Fig. 8.5.

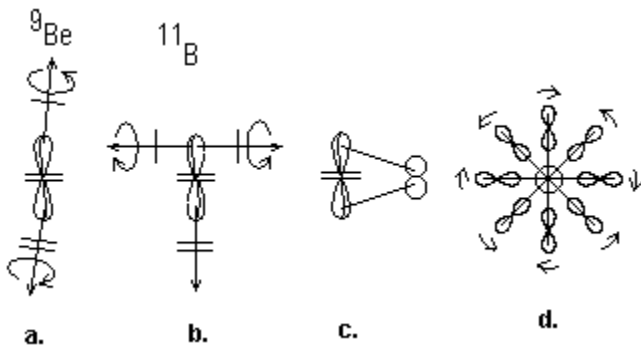


Fig. 8.5

The Hund's rule appears to be of four different types

The pairing in case a. and b. is a complimentary alignment of the two orbits, due to their common interactions. The interactions are result of the magnetic fields induced by the electron magnetic radius of their orbiting electrons, but kept inside the integrated Bohr surface. The arrows show the rotational direction of the electrons.

The electron pairing in case c. has a different physical aspect. In this case the free ends of the protons are approached and their electrons circle in a common orbit, passing through their clubs. (The electron trajectories are different only near the plane of the proton club.). The electrons must have opposite QM spin. This type of pairing provides electron bonding (EB) between protons connected to the opposite poles. In this type of bonding the protons are excluded from the principal valence of the element. This type of pairing corresponds to a Hund's rule applied for groups 11 to 17 of the periodic table.

The electron pairing in case d. corresponds to a completed proton shell. The paired electrons pass through a pair of GBclp bonded proton clubs. The orbital planes in this case are perpendicular to the orbital planes of EB bondings. The drawing plane

for the case in Fig. 8.5.d coincides with the equatorial plane of the atom. The orbital planes are slightly tilted to the equatorial planes due to the atomic helicity. In this case the neighbouring orbits are paired due to their proximity. This type of pairing will be additionally discussed in §...

Another feature for the cases shown in a. and b. is that the both electrons may have one and a same quantum numbers. In a first gland, it may looks that such condition is in conflict with the Pauli exclusion principle, but in fact it is not. The principle is formulated in accordance to the quantum mechanical model, where the electron kinetic energy and transition moment are associated with the emission of photon. According to BSM theory however, the photon emission is associated with the CL space energy around the proton. The latter is not identical to the electron kinetic energy, because in the nuclear proximity (inside of the Bohr surface) it redistributes much faster than the electron transition. Let to admit that both electrons of the pairing in case a. and b. have one and same same quantum numbers. They should have, however, different QM spins due to the orbital interaction. When one electron losing an energy falls in a lower orbit (following by a photon emission), the other electron will profit of this and will take a portion of this energy before the photon is emitted. Consequently the second electron now will have different kinetic energy. So the Pauli exclusion principle is still valid. In order to avoid some misinterpretation, when considering the BSM model the Pauli exclusion principle, could be reformulated: as: **Simultaneous emission of two photons from one atom, corresponding to one and a same transitions is not possible.**

Many isotopes are possible, but most of them are not stable for different reasons. The alkali elements starts always with a polar bonding. The element ^5Li (form by He and one D) is not a stable isotope, but ^6Li is a stable one. The reason is that the IG attraction between He and D is not strong enough in order to keep the GBpa bond between them. Adding one more neutron over the proton makes the IG stronger. But how the IG forces are able to overcome the E-field repulsion between the protons? From one side, the IG field manages to synchronise the oscillations of the internal positive RL(T) structures of the protons. In such conditions,

the induced in CL space E-field is displaced towards the club of the bonded proton. All polar clamped proton clubs then possess an unit charge, interacting with the charge of the polar electron. In such case the rule of charge unity is still conserved.

Polar region problem

Let considering the building of heavier atom as continuous growing process, by adding new protons. The IG field is able to control the charge unity in the polar region, but within some limit. If this limit is exceeded, one polar bonded proton will be separated and the balance will be restored. The effect is a radioactive decay. We may call this a polar region problem. This problem may be solved partly by adding a Deuteron or a Tritium instead of proton. The added neutrons pull up part of the IG field to the nuclear periphery. When adding only protons, the IG field concentration trend in the polar region is stronger, than adding Deuterons or Tritium. The increased IG field causes a CL space shrinkage, that is small, but still detectable, because it affects directly the CL static pressure and consequently the Newtonian mass. The detectable parameter in this case is the nuclear bonding energy.

- **The nuclear bonding energy is estimated by the Newtonian mass difference between the sum of masses of the protons and neutrons and the apparent atomic mass**

The polar region problem unveils when analysing the trend of the bonding energy in function of proton and neutron numbers and the X-ray properties. This is discussed in §8.6

The effect of polar region problem is apparent, but the mechanism is not enough investigated. One possible explanation is that in a large concentration of proton cores, the CL stiffness is increased beyond some level at which the IG field fails to redistribute the E-field lines and to keep the unitary charge.

Most unstable isotopes are result of the polar region problem. The stable elements have well balanced ratio between protons from one side and Deuteron or Tritium from the other. In the heavier nuclei, the polar region problem requires more neutrons in order to rarefy the field. For this reason the ratio between neutrons and protons gradually increases with Z number. While the Tritium as is unsta-

ble as a element, it appears stable when included in the nuclear structure of heavier elements. So protons with one or two neutrons provides a stabilizing effect. More than 2 neutrons over one proton however are unstable, and if such structure eventually appears, may lead to an radioactive decay by a neutron emission. In noble gases additional options appears for the neutrons to settle over the equatorial GBpcl type of bonds (see Fig. 8.4). The noble element ^{40}Ar , for example, has four such neutrons over its equatorial external GBpcl bonds

8.3.9. Atomic nuclear build-up trends

Let to describe briefly the build-up trends, following the Z increase in the periodic table. We will see, that build-up trend, following the Z number is characterised with shell structure made of consecutively added protons. In most cases, the protons are with one or two neutrons over their saddle. So in the build-up process, proton, deuterons and tritium are added. For terminology simplicity we will refer to protons, knowing that deuterons and tritium structures are inferred in most cases.

The He nucleus, as a most dens basic element, is in the centre of the polar structure. The first shell of the protons (deuterons) is built complying the rule for orbital pairing (one type of Hund's rule). The free proton clubs define the principal valence of the element. From group 15 to 17 the valence is determined by the free proton clubs that are not EB bonded (third type Hund's rule). In Nitrogen atom there is only one equatorial pairing, forming a weak EB bond. The bonded protons are excluded from the principal valence, so the Nitrogen has a principal valence of 3. At the Oxygen, the four protons obtain conditions for equatorial pairing. Instead of two weak EB, much stronger GBclp bonds are obtain, due to the perfect symmetry. The evidence of such conclusion comes from two different types of experimental data: the Z dependence of the first ionization potential (see §8.5 and Fig. 8.16) and the photoelectron spectra of molecules. (The latter will be discussed in Chapter 9.). At F atom, the Oxygen symmetry is broken and the EB type of equatorial bonding is restored. At Ne atom all the proton clubs get GBclp type of bonding and are excluded from any valence. In the same time the Ne gets a more compact structure than any

previous atom and the local lattice space gets a relatively larger shrinkage. This affects the nuclear mass according to a relativistic considerations, explained in Chapter 10. The Ne structure gets a completed rotational polar symmetry at 90 degrees. The transformation of GBclp to EB bonds is related to orbital transformation too, as shown in Fig. 8.5. The orbital planes for EB are close to the polar atomic plane, while the orbital planes for GBclp are close to the equatorial plane. In fact the orbital planes of the equatorial GBclp bonds at Ne intercepts the equatorial plane of the atom at small angles.

The second shell of protons (mostly deuterons), starting in Na and ended at Ar, follows a similar build up process. The equatorial structure is completed at Ar with an increased CL shrinkage effect (mass deficiency equivalent to a bonding energy). The deuterons in the second completed shell are very close to the deuterons of the first one. The most abundant isotope ^{40}Ar gets four neutrons symmetrically disposed over its external GBclp bondings (in the equatorial region). The Ar structure gets also a completed rotational polar symmetry with an alternatively arranged symmetrical structural features (at meridian steps of 45 deg).

The next shell starting from the element K grows initially by GBpa bonded deuterons in the two polar regions symmetrically up to ^{39}Co . The Cr atom is an exception from the ordinary growing trend. This is evident, when examining the oxidation states (O state - 70%; +2 state - 21%; +3 state - 38%; +4 state -3%). The lack of +1 oxidation state means, that there is not a free valence proton. The possible nuclear configuration, shown in the Atomic atlas is a four equatorial EB bonded structure of pair deuterons with He nucleus, polar connected to Ar nuclear structure. The three polar electrons in the two He structures have parallel orbits in a strong IG fields. So they may give a particular signature in the electronic spectra, which could be misinterpreted as a signature of a single electron in the external shell.

The build-up tendency is restored for a symmetrical polar growing at the element ^{55}Mn . This tendency is kept till Ni or Cu. It is controversial at which of both elements a jump to Ne like structure occurs. The correct assignment requires more detailed investigation of the differences between the

physical and chemical properties of the neighbouring elements. The ^{59}Cu atom, however, reasonably possesses a Ne like structure, but with EB type of bonds instead of GBclp bonds.

Following the growing trend, the stable isotope ^{63}Cu has one valence Deuteron (bonded by GBpc to the Ne like structure. The stable isotope ^{64}Cu has one valence Tritii instead of Deuteron. In Zn, two valence protons are GBpc bonded to the modified Ne structure. At Ga atom, the weaker EB bonds of the Ne like structures are converted to much stronger GBclp bonds. The bonded in such way protons are excluded from the valence. The build-up tendency after Zn, continues with bondings, attached only to the poles of the Ne - like structure. The growing trend provides valances similar like the previous raw of the periodic table, until the element Br. In the noble gas Kr all previous EB bonds are converted to GBplc. The orbit plane of the two electrons with opposite spins now is almost a parallel to the equatorial plane with a slight tilt due to the nuclear helicity. The external shell and a second Ar like structure is completed at the noble gas Kr. The both Ar - like structures are attached by GBpc bonds in their polar regions. The clamp attachment slightly change their equatorial radii. The Kr atom, however contains four more neutrons than the two separate Ar atoms. They compensate the polar region problem, mentioned above.

The 5th raw (Rb - Xe) follows generally a similar build-up tendency, but some differences appear. One of them is that the axial polar D (Deuteron) begins to get replaced by He nucleus. The first replacement is in Tc, but for this element only one polar D is replaced by a He nucleus. This asymmetry is perhaps the reason for the instability (radioactive) of the Tc. The build-up trend for Ru and Rh adds GBplc deuterons with EB equatorial bonds. . In Pd all equatorial bonds becomes of GBclp type so the bonded protons are excluded from the valence. From Ag to Xe the process is similar. For Ag, however, a possibility exists the D to be bonded also to the Ar polar structure.

The six raw begins at Cs with a polar GBpc attached deuteron, but after Ba, the polar bonding tendency is intercepted for the Lantanides build-up trend. The latter tendency is restored after all Lantanides are built, however, the bondings are not any

more to attached to the poles but to the equatorial points. So the growing tendency here has been changed, from a polar chain to an equatorial growing. This is dictated by the balancing conditions between the complex shape configuration, held by the the proximity IG field (leaking in CL space) and the distributed electrical fields of the protons.

All Lantanides grow by GBclp type attachments of protons (Deuterons) between the equatorial GBclp clubs of the two end polar structures. The attachment position initially follows the pairing rule, shown in Fig. 8.4.b., but only up to two protons, diametrically positioned. Then third proton (deuteron), at Pr, appears attached in the equatorial region of the opposite Ar structure and makes an EB bond with one of the first two attached protons. At Nd a new proton (deuteron) is attached in a similar way and makes a second EB bond. At Gd four EB bonds appear making the structure completely symmetrical with a rotational symmetry of 90 deg. This may be a feature related to the ferromagnetic property of Gd. The tendency of growing after Gd continues with EB bonds repeated at any second proton (deuteron). This keeps the principal valence between 3 and 4 (keeping in mind that two of the valences are contributed by the polar attached deuterons).

The structure of Gd is shown in Fig. 8.6. .

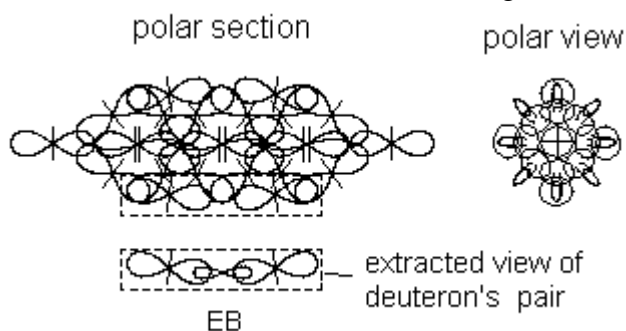


Fig. 8.6

Gd nucleus, EB - electronic bond

In the left projection, only the central elements, closer to the drawing plane are shown. Below the polar section the positions of the EB bonded Deuterons are shown. The EB bondings of these Deuterons are in this positions also in the higher Z atomic nuclear. The proton clubs are too apart and their EB bonds could not be converted to stronger GB bonds in the further build-up trend.

These bonds, however, could be broken in some chemical reactions, especially for the elements of the row 6 of the Periodic table after Hf. The higher oxidation numbers obtained for Au in cases of strong reagents could be explained by this effect. In Lantanides, some of the EB bonds could be also broken by strong chemical reagents. The EB bonded peripheral deuterons in the Lantanides are well axially aligned and their positions are preserved in the elements of higher Z number.

One of the most important feature of the peripheral deuterons in the Lantanides is that they are responsible for the alpha radioactive decay of the heavier elements.

The above made conclusion is valid for the naturally built elements. Some artificially built elements, by nuclear collision processes, may have very deformed or different structures. For this reason they have very short lifetime (in order of msec and sec).

The different build-up process of the Lantanides determines their different properties, not matching with the Periodic table row tendency of the other elements. One interesting feature is that the nuclear structure of Hf looks more completed than the Lu structure. At Hf the eight equatorial pairs of Deuterons are EB bonded. One feature, that may look strange, is that Hf exhibits only oxidation number of four. This could be explained if one EB bond only is broken. After Hf the growing tendency is by GBclp bondings to the equatorial proton clubs of the middle and one end polar structure. At Pt one polar deuteron disappears. At Hg the two polar deuterons disappear. They do not appear again and at Rn the external shell becomes GBclp bonded. One interesting growing transition appears between Au and Hg, and despite the neighbouring position in the Periodic table, their structures are quite different. The weak EB bonds of the Lantanides structures could be broken up to Rn and even at Rn. This may explain some chemical compositions of Rn. The polar section of the atomic nuclear structure of Rn is shown in Fig. 8.7. Only the central elements, parallel to the drawing plane are shown.

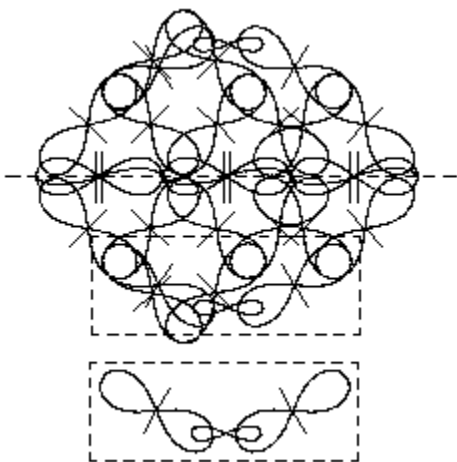


Fig. 8.7

Sectional view of Rn nucleus. For a 45° rotation around pp axis the sectional view is a mirror image

Below the sectional view of Rn nucleus a pair of deuterons is shown with their common positions. These deuterons are the sources of the He nuclei obtained by alpha decay.

The seventh row of the Periodical table starts again with polar GBpa bondings for Fr and Ra, but it is discontinued for the build-up trend of the Actinides. The growing process in the Actinides is different than the Lantanides. The Actinides grow by GBclp bondings to the adjacent two equatorial proton clubs, in the equatorial space left over from the previous 6-th row. The growing trend of the Actinides and the following transuranium elements tends to form a more spherical shape of the nuclear structure.

8.4 Experimental data in support of atomic nuclear structure according to BSM.

8.4.1 The polar region effect and a proton to neutron ratio

The polar region effect can be investigated if making a plot of edge levels of mass attenuation coefficient of X-ray data in function of Z , then fit to a polynomial and observe the residuals. The residuals, obtained in this way, look differently for the internal and the external shells. Careful investigation provides indications that: the neutrons are added in the periphery; the neutrons and the protons affect differently the internal and the external

shells. Such plot for K edge levels of x-ray mass attenuation coefficients towards the Z number is shown in Fig. 8.8.

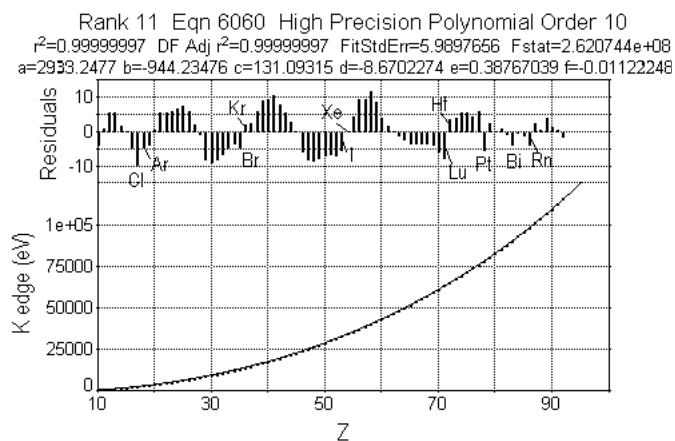


Fig. 8.8

The plot starts from $Z = 10$, instead of $Z = 0$, because the residual fluctuation depends of Z also statistically. The statistical error, however, is of random origin and is easier identifiable. For $Z > 10$ it is significantly reduced. Analysing the residuals, we see larger positive jumps in the transitions from the group 17 to the group 18. This is due to the compactifying the external shell, when all eight proton clubs get GBclp type of bonding. The IG field is pull out to the equatorial region, causing a decreases of the CL shrinkage in the polar regions. Another two interesting features are observed. The element Pt gets a negative jump. This is a result of losing one polar Deuteron. The next atom Au, although, gets a positive jump. **This shows that its external shell containing 8 protons (Tritii for ^{197}Au) gets GBclp type of bonds and therefore it is completed. This explains why Au is a noble metal.** The Au atom still has one valence proton that play important role in a solid state. Otherwise it would be a noble gas. Examining the oxidation number we see that it has a large first oxidation state, a very small 3rd and insignificant 2nd one. The 3rd and 2nd states comes from braking one of the weak EB bond from the of underlying EB bonded deuterons in the Lantanides shell. The Lantanides type of bonds, can't be never converted to GB bonds, because the distance between the proton clubs is large. Examining the spatial nuclear structure we see that these bond are below the external

shells and could be broken in very special conditions. From the change of the growing tendency between Au and Hg one interesting conclusion could be made:

Let suppose that the valence deuteron of Au is removed but the nuclear structure is not refurbished. Then it will have the same number of protons like Pt, but its nuclear configuration will define different chemical and physical properties. Its properties could be rather similar to those of the noble gases. It is not sure, however, how stable will be this element.

8.4.2. X ray properties of the elements

It has been considered so far (in the contemporary physics), that the X - crystallography is applicable for studying the structure of the solid crystals made of atoms, but not the atoms themselves. This concept is a result of the consideration that the atomic nucleus is very small. The proton radius, for example, has been considered to be in the order of $1E-15$ (m). The BSM theory, however, unveils that the proton has a shape of a Hippoped curve (close to the figure 8) with external dimensions of $(0.667E-10 \times 0.1925E-10)$ (m), with a core thickness of $7.841E-13$ (m). Then the nuclear structure is also possible to be studied by the X rays technic including the X ray crystallography.

8.4.2.1 X ray transmission in function of X-ray energy

A narrow beam of monoenergetic X-ray with an incident intensity I_0 , penetrating a layer of material with a thickness t and a density r , emerges with an intensity I given by the exponential attenuation law. $I = I_0 \exp(-(\mu/\rho)\rho t)$. The grouped parameter ρt is called mass thickness, while μ/ρ is known as a mass attenuation coefficient. The following relation is valid between these two parameters

$$\mu/\rho = \frac{\ln(I_0/I)}{\rho t} \quad (\text{cm}^2/\text{g}) \quad (9.1)$$

The mass attenuation coefficients are specific for every element. A good reference source, where the X-ray data are summarized in tables and plots is provided J. H. Hubbel & S. M. Seitzer, (1998). They are presented usually as tables and plots of μ/ρ as a function of the x-ray energy, together with

experimental data. The experimental data usually use the total attenuation. They are collected from a large number of published experiments, provided from the beginning of 19th century. Between the most characteristic features of the plots are the absorption edges, characterized by a sharp change of μ/ρ at some particular energies. This is illustrated by Fig. 8.9 showing the experimentally measured total attenuation of ^{29}Cu (included in the data source given by J. H. Hubbell, 1971).

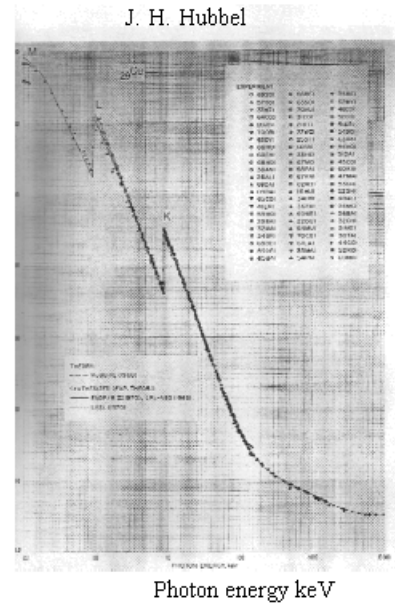


Fig. 8.9

Experimentally measured total attenuation for ^{29}Cu

It is evident that the edges are tightly connected with some shell structure. Theoretical models for explanation of the edge effect exists. They use multilayer modelling with a Fresnel and Bragg reflection effects and provide good interpolation of the experimental data. The detection of the atomic shell structure by X-ray methods is not a discusional fact. But one question arises: If the atomic nuclear is in order of $1E-15$ m, how the internal structure will be detected with wavelengths of order of half of angstrom, for example? In this case a contradiction appears between QM model of the atoms and models relying on experiments. According to the QM model of the atom, the hardware structure of the atoms must be determined by the electron orbits. But how they are kept in very ordered positions orbiting with a relativistic velocity without radiation of energy? How do they resist to

any external stress and the penetrating X-rays? These are simple physical questions for which the QM model does not have answers.

The explanation of the transmission behaviour of the solids, according to BSM, is a following:

The observed edge zones of the mass attenuation coefficient are caused by the refracted and reflected X-rays from the quasishrunk CL space inside the Bohr surfaces. Inside of this surface the shell arrangement of the protons & neutrons (mostly deuterons) causes CL zones with a different degree of shrinkage and a complex shape. The additional effect of Brag reflection, which is defined by the atomic arrangement in the crystal structure will provide additional signature, which will be superimpose on the above mentioned effect.

The quasishrunk space exists inside the Bohr surface, due to the E-field spatial distribution (discussed in §7.6, Chapter 7.). This space namely behaves as a gradient optics for the x-rays.

In order to show the edge effect, a simple analogy is made by using an example of two concentric optical layers with different refractive indices. For this reason an optical ray tracing is provided, as illustrated by Fig. 8.10. The layers are shown as lenses having concentric radiuses, but different indices of refraction. The internal lens L1 has $n = 2$ corresponding to a more shrunk space, while the external L2 has $n = 1.5$. An optical ray tracing program is used and the result is evaluated by annulus scanning aperture.

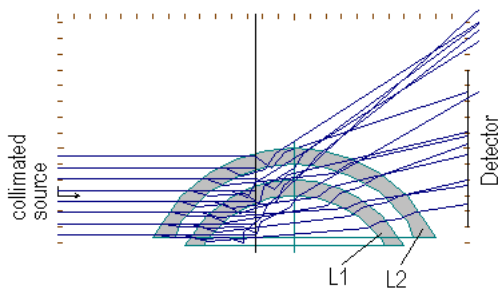


Fig. 8.10

Ray tracing is provided for a case of one and two lenses. The results are shown in Fig. 8.11, where radiometric analysis with a scanning

annular aperture for a case of two lenses is also shown.

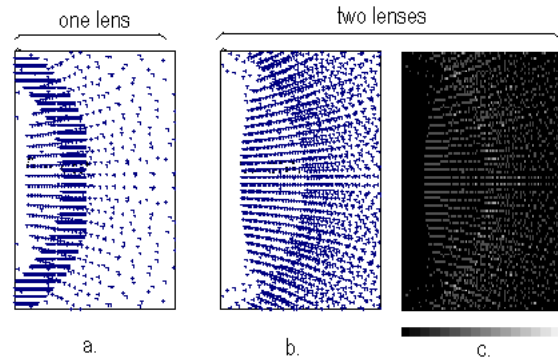


Fig. 8.11

- a. is a spot diagram in a case of one lens only;
- b. is a spot diagram for a case of two lenses and
- c. is a radiometric analysis with a scanning annular aperture for a case of two lenses

In a case of one lens, a deep valley appears. In the case of two spherical lenses, the appearance of one sharp edge is evident. In the atomic case, the shells will behave as optical layers with gradual index, but the edge effect could appear in a similar way. If changing the wavelength, the index of refraction will change and the edge will be shifted respectively. However, this is still a spatial edge effect. To explain the edge effect of the mass attenuation coefficient, additional consideration should be taken into account. This is the atomic positions inside the solid cell, where the atomic polar axes may have different orientations, but following a strictly determined order. Then in the case of symmetrical angular distribution (as in case of one lens), the transmitted total flux will have symmetrical behaviour around the wavelength of the maximum transmission. In the case of asymmetrical angular distribution, (corresponding to the example with two lenses), the transmission in function of the wavelength will have also asymmetrical appearance. Then the analogy with two or more lenses will be valid for the proton shell, which gets a completion at Ar. The proton shell, however, begins to obtain a focusing effect when getting EB bonding. In the optical example, this shell could be associated with the lens L2. The lens L1 will be associated with the He nucleus.

The analogy could give only a rough impression of the picture inside the solid crystal. In the real case the spatial ray distribution is quite more complex because of number of factors: a gradient index change, the proton shape and the spatial positions of the atoms in the solid crystal and so on.

Investigating carefully the X-ray transmission and the characteristic X lines associated with the shells (next paragraph) we may conclude:

For X-ray range between 1 KeV and 100 MeV:

K edge corresponds to the shrunk CL space around the proton shell, which shell gets a completion at Ar atom

L edge corresponds to the shrunk CL space around the proton shell, which shell gets a completion at Kr.

M edge corresponds to the shrunk CL space around the proton shell, which shell gets a completion at Xe.

N edge corresponds to the shrunk CL space around the equatorial proton shell, beginning at Ta.

For X-ray range between 100 eV and 1 KeV:

The edge frequency depends on the crystal geometry and the spatial positions of the valence protons

Discussion about **additional features:**

The top of the L edge begins to appear slightly doubled from Cu. This could be explained by the CL shrinkage, that appears for Cu as a result of EB bondings. The doubling increases continuously, because the proton arrangement around the two end polar structure and the middle one become different .

The N edge never gets the sharpness of the previous edges. This is an equatorial proton shell, following different build-up principle. At Rn two similar equatorial shells exists, but the Actinides protons grows between them.

8.4.2.2. Characteristic lines of X ray spectrum

The spectrum of the characteristic x-ray lines is strongly related to the transmission edge position. Lot of experimental data are accumulated mainly in the first half of 20th century. Following the energy increase order, the lines are annotated as

a, b, g and so on. For many elements the *a* line is measured as a doublet. The energy condition for appearance of these lines requires the activation energy to be above a specific threshold value equal to the line quantum energy. This energy is little bit below the transmission edge energy. Ordering the line set by the wavelength, the *a* line appears with a longest wavelength, and strongest intensity. **However, one very interesting effect exists with the following features: 1) Applied monochromatic X-ray radiation (activation energy) in a broad spectral (energy) range leads to emission of spectral lines with stable wavelengths; 2) The increasing of the activation energy leads to an intensity increase of the characteristic lines with a preserved intensity ratio between them.**

Similar effect does not exist in UV, VIS and IR spectral range.

At the transmission edge energy, the intensity of the characteristic lines begins to grow much faster. This effect was observed and extensively discussed by D. Webster (1916). In his and other discussions in that time, an energy storing mechanism is thought to have place. This energy storage mechanism works for the time the activation energy is present. The reason for such admittance is the independence of line wavelength from the wavelength of the activation monochromatic energy. In the same time the increasing of the activation energy does not show a discontinuity. In Webster's experiment the Rh lines: *a* (doublet), *b* and *g*, are studied for a pretty large range of the activation energy (from 20 to 32 KeV for a line). The plot of the *a* and *b* lines with the fluorescence radiation is shown in Fig. 8.12.

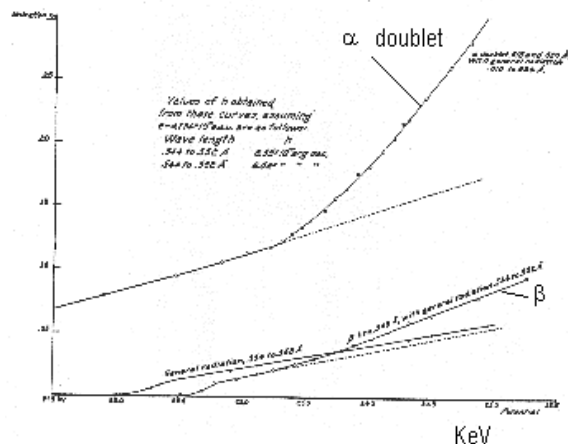


Fig. 8.12

The beginning of sharp intensity growing is carefully investigated by Webster, and found to be 23.3 KeV +/- 1%. This value is very close to the edge energy for Rh, that has a value of 23.22 KeV.

The physics of the energy storage mechanism has not been explained so far.

8.4.2.3 Characteristic x-lines and energy storage mechanism according to BSM

For UV, VIS and IR spectral range, the photon emission and absorption is a result of electron transitions between different quantum orbits. So this is atomic type of photon emission and absorption process. The **weak electron system oscillations** serves only to comply to the quantum type of motion.

The mechanisms of X-ray photon emission and absorption is quite different than the atomic type. The photon emission in X-ray region is due to **strong electron system oscillations**. The electron motion only could affect the propagation of the emitted photon in the external CL space. The photon emission process was extensively discussed in Chapter 3. From the analysis of the experiments we may conclude that:

- **The electron system can emit X-ray photons during its orbital motion around the proton club.**
- **The X-ray radiation is not an electronic transition process between the shells. The emitting electron does not change the quantum orbit**

Possible explanation of X -ray activation of orbiting electrons by BSM: The X-rays are able to penetrate inside the quasishrunk CL space (which is inside the Bohr surface) due to their shorter wavelengths. The characteristics lines are located around the transmission edges. For well defined sharp edges they are stronger. This means that the activation radiation is able to penetrate in the shrunk CL space and may affect the electron spin momentum. Then a special interaction process may occur, when **the electron orbital length is an integer number of radiation wavelength (condition A)**. When this condition is fulfilled for the current electron orbit, the activation energy could affect the SPM vector of the space swapped by the electron magnetic radius. Then the electron has to

fulfil simultaneously two quantum conditions: 1) keeping the same quantum number (from the short magnetic line condition (see section 7.7.1, Chapter 7); and 2) meet the new modulation of SPM vector. The first condition is related with the positron-core oscillations, while the second one - to the electron spin rotation. The energy causing the discrepancy between the two quantum conditions is much larger in comparison to the quantum time conditions in CL space without external energy. **So this energy causes stronger oscillations between the electron shell and positron.** From Chapter 3 we know, that such oscillations lead to emission of X rays.

X-ray energy storage mechanism

There is a second feature. The continuous range of activation energy means that the described process should be satisfied for some limited but continuous range of wavelengths. The possible explanation, is that the different wavelengths are distributed in the quasishrunk space around the proton core. The Balmer model in Chapter 7 shows good results for linear dependence of the quasishrink factor from the distance r (between the electron orbit in the circular part and the proton core). The refractive index is a reciprocal to the quasishrink factor and also is gradual (but not linear). In conditions of gradual refractive index, the applied monochromatic radiation may be converted to standing waves, occupying volume with finite thickness around the proton core. **Then the condition A, could be fulfilled for a volume adjacent to the quantum orbit, but from the side to the proton core.** This waves could be able to transfer their energy to the space volume of the current quantum orbit, due to the lattice stiffness gradient. The energy transfer is from larger to smaller stiffness. In such case a finite range of wavelengths could be able to transfer their energy to the electron.

This kind of energy transfer could be possible due to the non linear factor: the intrinsic gravitational field around the proton core. We may call this effect **X-ray Energy Transfer Mechanism (XETM)**.

The spatial position of the XETM in respect to the proton's core is shown in Fig. 8.13, where a

section across the quasishrunk space around the proton club is shown.

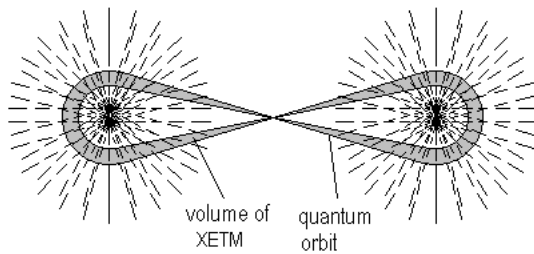


Fig. 8.13

Orbital range with conditions of standing waves
The range is around the GBclp bonded protons

The volume, where the XETM could function is shown by gray level. It is below the quantum orbit. The quasishrunk CL space is around the two GBclp bonded proton clubs. The position of the current electron orbit is also shown.

One question arises: Does this process possess a finite time constant, in order to be considered as an energy storage mechanism?

The available experimental data does not allow a definite answer, but the possible time constant may be related with the modified CL time constant for the range of the quasishrunk space, where the effect may take place.

Characteristic line splitting

One important feature found in the experiment is related with the characteristic line splitting. Only doublets are observed. The author of BSM is not aware of observed triplets or multiplets. To explain this feature, having in mind the X-ray emission mechanism, we will use the Fig. 8.5.d. The drawing plane coincides with the equatorial atomic plane and shows the orbits around the GBclp bonded proton clubs of a completed proton shell. (Every internal shell is completed). As a result of the orbit proximity, they could be influenced each other. The lowest energy they could get according to the Hund's rule is when they are paired. The arrows show the electron motion for this pairing. The applied radiation penetrates inside the Bohr surface of each proton guided by the proton helicity. While the proton helicity is one and a same, the electron motion in the neighbouring orbitals is opposite, because of the orbital interaction. For this reason the

line is doubled. Then the following conclusion could be made:

The fact that the line doublet appears clear and well separated when applying external radiation means that:

- all orbits in the shell obtain the same principal quantum numbers
- half of the orbits possess a right handed and another half - a left handed QM spin
- the above two conditions are valid only for completed proton shells with GBclp type of bonds in the equatorial region

From the above made conclusions, it follows also, that the simultaneously observed different lines come from different atoms. It also means, **that the lines could be split only in doublets.** This latter statement is in agreement with the observational data, but in contradiction with the methods for calculating the characteristic lines, that is based on electronic transition between the shells.

There is a lack of experimental data showing close triplets or multiplets, while a lot of doublets are observed. The multiplets if existing should appear very close, like the doublets. They should be not confused with lines from other quantum orbits. The elements after La, although, could exhibit more complex line structures, because the condition for absence of additional equatorial bondings is disturbed. In such case W, for example, shows a larger number of lines, but only one doublet is identified (A. Compton, 1916).

The pairing effect makes the characteristic lines to appear quite strong. Using this feature and XETM effect, X-ray lasers could be built.

Discussion:

It is a question if the *a* characteristic line is emitted from the the lowest or higher level orbit of the series. When the activation energy scans from lower to higher energies, the order of the line appearance is *a, b, g*. Then the *a* line should correspond to the most external, from this set of three orbits. But then its strength will be strongly dependent on the temperature. The question could get an answer by suitable temperature data set.

8.4.2.4 Laue patterns

The Laue patterns are diffracted images, when a solid structure is radiated by collimated X-rays. The solid structure should be carefully cut on order to match the particular crystal plane. Such images of pure elements are of particular importance. The interpretation of the results is complicated, due to the large CL shrink factor around the proton and neutron cores. But the polar symmetry is helpful in order to unveil some structural features. In this case the back-reflection and transmission Laue patterns are useful.

In the back-reflection patterns the most intensive spots are due to the external shell protons (Deuterons). But some weak patterns are from the nearest internal shell. The polar axis of the atoms may have different orientation even in one cell. In a proper orientation of the crystal, when the polar axes of group of atoms become normal to the image plane, the correct angles of the proton positions in the atomic equatorial plane will give diffractive spots.

From the Lauer Atlas, by Eduard Preuss et al., (where for some elements the pattern only is given), one may find that:

- The rotational polar symmetry of 45 deg (corresponding to 8 protons in a polar view) appears for: Ga(010), In(100), In(001), -Sn(001), W(100), Np(001), Np(100).

- For Mg the “45 deg pattern” is missing and this is a good sign, because it does not have 8-proton shell.

For elements with Z number larger than 12, the “45 deg” pattern may appear, because only one proton in a “45 deg” position could be able to contribute to the Laue pattern (due to the different atomic positions in the neighbouring crystals).

The transmission Lauer patterns are also useful. Fig. 8.14 shows a transmission pattern of Fe under stress, provided by Wadlund (1938). The 45 deg feature has a strong appearance. The origin of the radial lines has been in discussion in the time of the experiment, but not reasonable explanation is obtained. Now, having in mind the BSM model, the stronger appearance of the radial stripes in the transmission pattern are easily explainable. The stress may cause deformation of the Bohr surfaces, but the polar symmetry is preserved.

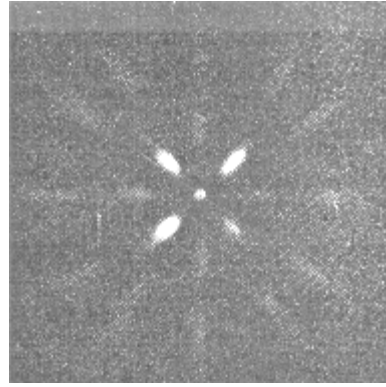


Fig. 8.14
Laue photograph of compressed iron crystal. Courtesy of Wadlund (1938)

Another very interesting experiment provides the transmission pattern of aluminium, in cases of polychromatic and monochromatic X-ray beam, at room and at elevated temperatures. The images are shown in Fig. 8.15.

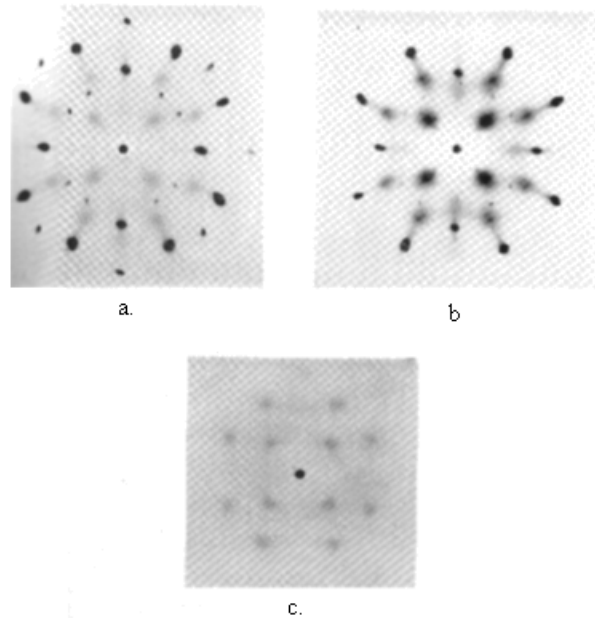


Fig. 8.15
Aluminium, X-rays parallel to [110] vertical
a. room temperature; b., 500° C; c. monochrome Ag Ka radiation. Courtesy of G. Preston et al. (1939)

The spots whose appearance is stronger at elevated temperature has been a subject of hot discussions at the time of the experiment, but without good explanation. According to the BSM, these spots are due to the characteristic line radiation. At elevated temperature, the spots are quite more intensive and diffused than at the room temperature. At monochromatic radiation, the spots become

smaller but well defined. This corresponds to an increased contribution from the characteristic lines. The fixed and symmetrical locations of the spots are in good agreement with the BSM atomic model and the concept of the X-ray radiation, described in the previous paragraph.

The X-crystallography technique could be very useful for confirmation of the unveiled atomic structure. The diffraction image is a result of two major factors: the focusing property of the CL space around the proton clubs and the Bragg conditions caused by the repeatable surfaces. However, it is necessary to distinguish the spots contributed by the proton shells from those provided by the atomic positions in the crystal. A proper orientation of the crystal is necessary in order to make the polar axes of group of atoms normal to the detector plane. One very useful feature would be the X-ray source to be monochromatic with an option of variation of the wavelength and the beam intensity. In such case the spots contributed by the completed proton shells could be selectively observed and identified by the appearance of the characteristic line radiation. The azimuthal positions of electron orbitals also could be identified.

8.5 First ionization potential

The trend of the first ionization potential in function of Z number for the first 21 elements from the Periodic table is shown in Fig. 8.16.

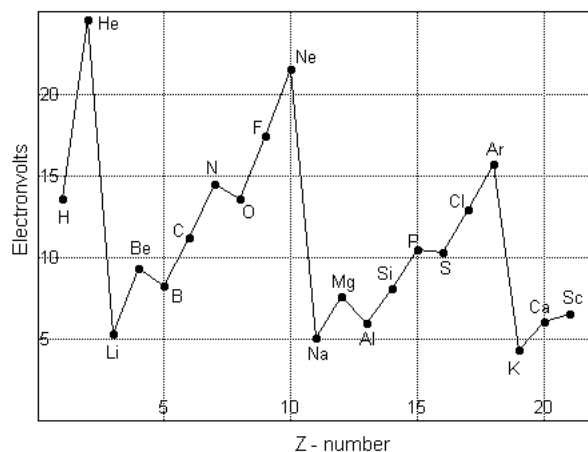


Fig. 8.16
First ionization potential of elements
for $1 < Z < 21$

The rising trend for the elements in one row of the Periodic table is explainable by the increasing number of the protons in the external shell. The sharp potential drops for Li Na and K elements indicate the beginnings of new shells. Proton shell are compactified at Ne, Ar, Kr and Xe. In the same time, all electron orbits in the completed shell become closer to the central region and their orbital planes are almost parallel to the equatorial atomic plane. The orbital planes of the polar electrons are also parallel to the equatorial plane. For this reason a removing of electron from the inert gas up to Rn requires a larger ionization energy. For Rn the first ionization potential is much smaller in comparison with the inert gases with lower z number, because the electron might be extracted from the weaker lanthanides EB bonds.

A less strong decrease of the ionization trend appears between Zn and Ga. This indicates that the EB bonds of the four previously bonded protons are converted to GBclp bonds. The attached structure becomes identical to a Ne structure. Consequently, the protons of this structure are completely excluded from the valence of the element. A similar trends exist between Cd - In and Hg - Tl. This means that a similar effect takes place.

In the rising trend of the ionization energy within the first few rows of the Periodic table, the following anomalies are observed: Reversing of the potential trend between: Be - B; Mg - Al; N - O; P - S; As - Se. The Be - B trend indicates, that Be has two bonded protons at one and a same polar region, corresponding to one type of Hund's rule pairing. (The pairing in fact is between the electron orbital planes, but they influence the proton position in the nucleus). The next bonded proton for B is attached to the opposite pole. So it slightly disturbs the proton pairing obtained at Be. This facilitates the removing of electron from the latter proton at B.

A smaller reversal jump occurs between N - O and P - S. This might be also a conversion of EB to GBclp bonds. The possible explanation of the ionization potential drop is a following:

Let to analyse the magnetic field orientations, considering the plane of the electron orbits, for simplicity. In Nitrogen, the plane of the three valence orbitals (determined by the valence proton) are (approximately) normal to the equatorial plane.

The planes of the two electrons from the equatorial EB bonds are also approximately normal to the equatorial plane. Due to the proton twisting the both type of orbits are not completely normal between themselves. So some interaction could exist. In the Oxygen atom, the two GBclp are completely symmetrical and the valence protons also. Then the corresponding orbital planes are also symmetrical. The equivalent plane of the orbits of the GBclp could be considered exactly parallel to the equatorial plane. The equivalent planes of the two symmetrical valence orbits (at the proton's free clubs), however, appears always at angle in respect to the equatorial plane, so the interaction effect should be smaller. This means, that the valence electron should be ionised by a smaller energy. The possible configuration of Oxygen atom is illustrated in Fig. 8.16.B by two views: A and B..

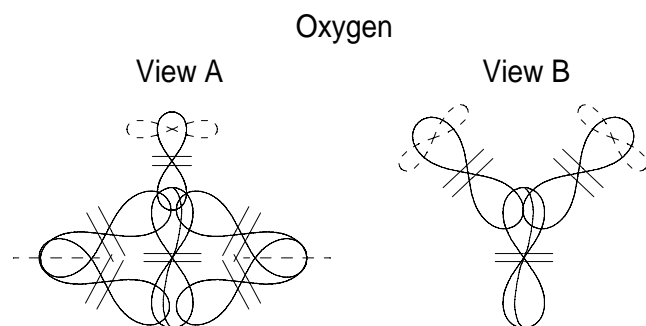


Fig. 8.16.B

The analysis of the photoelectron spectrum of of the atomic oxygen, according to BSM, is also in agreement with the shown configuration (especially the autoionization features of the oxygen obtained by excitation with the strong neon line at 73.6 nm, see Fig. 9.43.A in Chapter 9 and the BSM explanation).

The same effect should be valid for the atoms of the same group: S, Se Te. For the group of halogens (F, Cl, Br, I), the number of the equatorial bonds are three. Three EB bonds are able to generate closed magnetic lines around the polar axes. So the equatorial proton pairing is by EB bonds. This means a larger ionization potential, according to the above analysis. This is also in agreement with the plot shown in Fig. 8.16.

8.6. Atoms at different aggregate state of the matter

In a gas phase of the matter the atoms have a full freedom of motion, while the external protons (deuterons, tritii) has a limited freedom of motion relative to the atomic nuclear core. In the liquid phase the average distance between atoms (molecules) is a constant, but the protons still have some freedom. It is known that so called hydrogen bonds play a role in the liquid water. If taking into account the limited angular freedom of the valence protons (deuterons) and the orientational freedom of the molecules this is completely understandable for the BSM atomic models.

In the solids the protons (Deuterons, Tritii) lose their freedom of motion, because they provide the interconnections between the neighbouring atoms in the crystal. This connection is different for the insulators and for the metals. In both cases the atoms are arranged in a crystal structure.

Even the amorphous solids (like glasses) may have a crystal structure in their not oriented domains.

The crystal structure of the insulators is different than this of the metals.

In the insulators all the valence protons of one crystal cell are connected to the valence protons of the neighbouring cell by EB. As result of this, there are not free electrons in the solid structure. The distances between the atoms in this way are usually larger and the intrinsic gravitation between the bonded protons (deuterons) is smaller. In the space between atoms a CL exists, but with local variation of its parameters, influenced by the atomic structures. This makes a suitable condition for free passing of EM waves and light, but with a reduced light velocity in comparison to the vacuum due to the slightly changed proper resonance frequency of the CL nodes.

Metals When analysing the differences between the external proton shells of the metals and insulators (for single elements only) we see that:

(1) There is a larger abundance of GBclp in the equatorial peripheral range for the metals, than for the insulators

(2) The GBclp of the completed polar structure Ar is always uncovered by valence protons

(3) The number of completed Ar structures increases (up to 3) with the row number of the Periodic table.

(4) The number of metals in the transition elements of the Periodic table gradually increases. So the boundary between the metals and semiconductors in the Periodic table is not a vertical line but a diagonal: Zn In Pb (Bi).

It is evident, that the number of the equatorial GBclp bonds play a role in the crystal cell of the metals. These bonds possess larger IG fields and may attract and align the neighbouring atoms. This conclusion is experimentally confirmed by the BSM interpretation of the observed gold crystal structures by T. Kawasaki et al. (2000). For this purpose the group of Kawasaki used a new developed transmission electron microscope with a resolution of 0.6 Å (0.6E-10 m).

Fig. 8.17 shows the transmitted pattern for 15 nm thick Au film by successive vacuum deposition onto Ag layer (200 Å thick). The comments for Fig 2 (from the paper) are from the authors. The images (a) and (b) correspond to two different crystal planes.

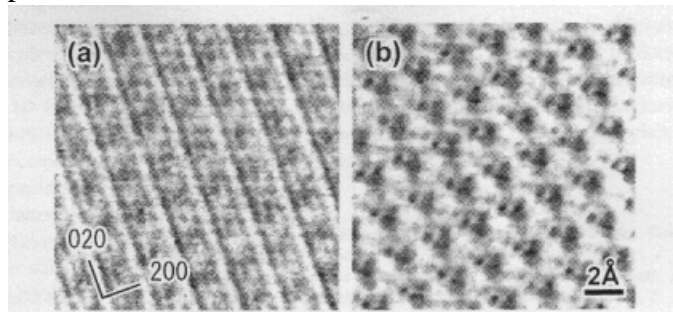


FIG. 2. (200) lattice fringe ($d=2.04 \text{ \AA}$) images of a Au(001) thin film: (a) 1/3 spacing fringes formed from $(\bar{2}00)$ and (400) reflections; and (b) fringes formed from many high-order reflections. The Fourier transform of the micrograph extends to $\sim 0.5 \text{ \AA}$

Fig. 8.17

Courtesy of T. Kawasaki et al. (2000)

BSM interpretation: Crystal (lattice) image of Au thin film in two crystal planes

While the Kawasaki group interpretation relies on the QM concept, the interpretation according to BSM concept is different.

According to the QM concept: The image is a fringe pattern contributed by the electron clouds

According to the BSM concept: The fine structures of the observed pattern are contributed by the electronic configuration, which comply to the nuclear structure, because all the electrons are around GB type of bonds. Consequently, the fine structure details of the observed pattern carry a signature of the atomic nucleus of the Au (gold) atom.

The shape and the configuration of Au atom, according to BSM is shown in Fig. 8.18, where **a.** is the polar section and **b.** is one polar view. In the polar section, only the protons intercepted by the section plane are shown for clarity.

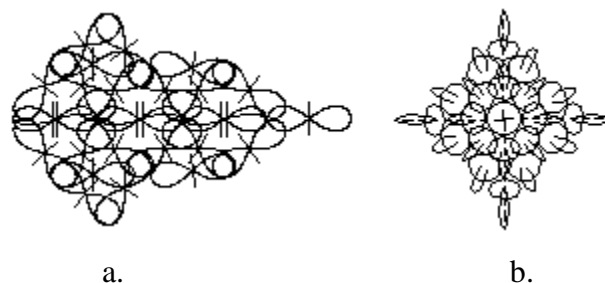


Fig. 8.18

Au nucleus: a. - polar section; b. polar view

The single proton (Deuteron) in the left side of the view **a.** is the valence one. The valence electron (not shown) is orbiting around the free proton's club. From Fig. 8.18 we see, that the shape and dimensions of Au nucleus are completely determined, when knowing the proton dimensions. This gives a possibility to explore the possible arrangement of the Au atoms in different crystal planes using a real scale. Fig. 8.19 and Fig. 8.20 provide possible synthesized images corresponding to the crystal planes for the images in Fig. 8.17. The scales are in dimensions referenced to the proton length.

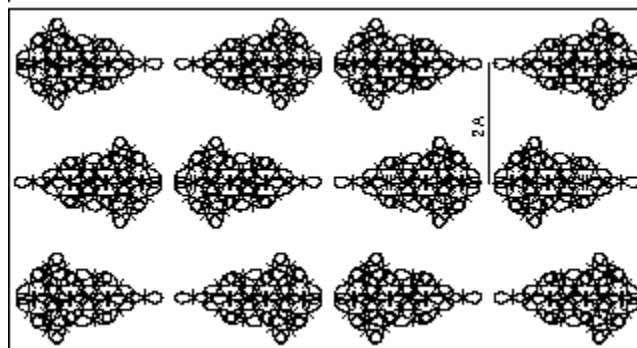


Fig. 8.19

Synthesized image of Au(111)

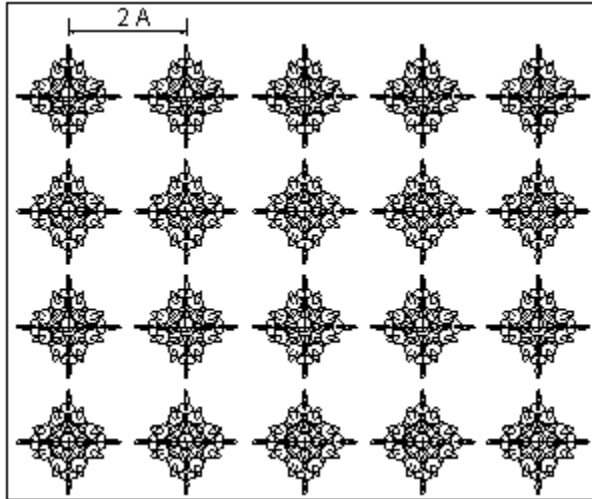


Fig. 8.20
Synthesized image of Au (111)

Comparing the synthesized images to the experimentally observed, we see, that the dimensions between atoms and patterns match very well, only the plane orientation is rotated. From the image in Fig. 8.19 we see, that the valence protons are adjacent, and consequently connected by EB bond. In the opposite side of the nucleus, however, EB type of bonds are not possible and the possible connection is only by IG forces or this is a kind of IG bond between the separate atoms. This corresponds to one type of the Wan Der Wall forces. The alignment between neighbouring rows is possible only by the IG forces between GBclp bonds in the equatorial region.

Fig. 8.21 shows another image with different resolution from the same authors (T. Kawasaki et al. (2000)). The angle α between the line patterns is not 45 deg, but 40 deg. The same angle appears also in Fig. 8.17. This feature indicates, that the cell of four adjacent atoms does not has a rectangular shape, as shown in the synthesized image of Fig. 8.20. The cell is slightly rhomboidal. The only possible nuclear feature that cause the rhomboidal shape of the cell is the nuclear twisting along the polar axis. This twisting, however, could influence the shape of the cell only by the interaction between the equatorial GBclp bonds of neighbouring atoms. Then we again come to a conclusion, that pure IG type of bonding exists between the atoms in the solids

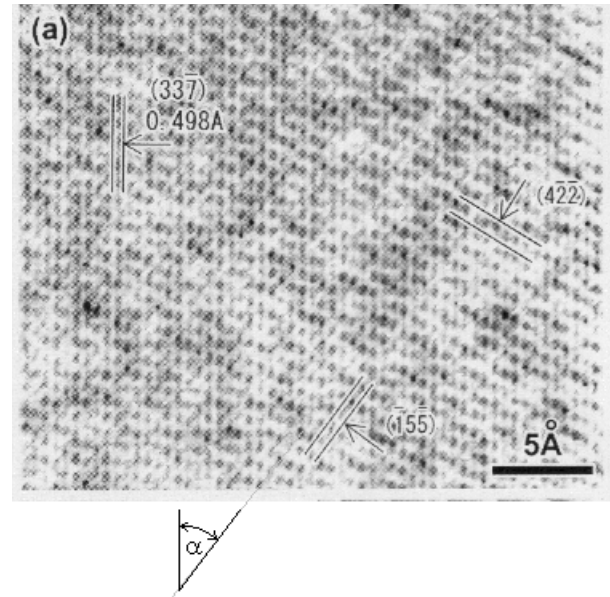


Fig. 8.21
Electron micrograph in a Au(111)
(Courtesy of T. Kawasaki et al. (2000)
Note: The angle α below the image is
is added by the author of BSM

The GB bondings between atoms become active, if the atoms are in enough close distance. The EB bondings probably counteract for such proximity keeping the atoms apart, even if their polar axes are aligned. The EB bondings starts from the group 11 of the Periodic table and their number progressively increase in the halogens. The boundary of the metals - semiconductors however is not vertical from the rows 4 to 6, but follows a diagonal, because the elements of every consecutive row after number 4 have one more additional Ar like structure with their GBclp bonds.

One additional question should be replied for the metals: ***How the “gas” of free electrons is formed in the metals?***

When the atoms are separated, like in the gas phase, every electron is orbiting around its proton.

In the solid phase of the metals, some electrons obviously should be permanently free due to some mechanism. Using again the example with the Au crystal structure, we see, that every four proton pairs with EB are in close distance. The polar proton (deuteron) have some freedom of angular motion. By small tilting of this proton it is

possible every four pair of EB bonded proton to form a **cluster of closely spaced protons**. The increase IG field of this cluster might be able to synchronize the dynamical interactions between the internal RL(T)'s of the proton shells and to control the common charge of the cluster to 2 unit charges, for example. Then this volume will be served by pair of electrons with different QM spin. We may call this hypothetical effect a **free electrons effect**. As a result, six electrons will become free, contributing to electron gas formation. So the free electron coefficient in this case will be 1.5 electron per atom. In other metals, the free electrons effect is also possible, when more than two valence electrons are in proximity. The effect is possible not only for valence electrons, but also for EB protons (of one atom). The pair of EB bonded protons are not necessary to be unbonded. In proper orientation of the atomic nuclei they may become close enough in order to form a proton cluster and to allow a free electron effect. This conclusion could be confirmed by the example with the electrical conductivity for Fe and Cu. Their possible cell configurations are shown in the Atomic Atlas. Fe and Cu, both have almost the same mass density, but very different electrical conductivity. In the same time Fe has more valence protons, than the Cu (only one). The copper, however, has four EB proton pairs, while the iron does not have such pairs.

From the above made analysis it becomes apparent that the metallic feature of the elements appears only when they are in a solid aggregate state.

For the semiconductors the external protons are closer in comparison to the isolators, but not closer enough to form clusters like in the metals. When the applied field exceeds some level, some electrons could migrate from a local atomic orbitals to orbitals of neighbouring atom.

The space between the hadrons involved in the nuclei (protons and neutrons) is a CL space. The average internuclear distance, normalized to the nuclear size, is a largest one for the insulators, a smaller one for the semiconductors, and a smallest one for the metals. The non spherical shape of the atoms and the internuclear bondings are behind the different properties of the different crystal planes. This is apparent by their Laue patterns. Different metals have different hadron concentration,

which modulates the CL space to a different level. So the CL space inside the solids exhibit a spacial nonuniformity even for a crystal structure from one and a same element. Such uniformity may increase significantly if the solid body contains impurities. The obtained in a such way local nonuniformities play a significant role in the superconductivity state of the matter (this was mentioned in Chapter 4). Compounds of different elements, mostly metals may get larger local nonuniformity. They are of increased interest in the area of high temperature superconductors.

8.7. Nuclear magnetic resonance applied for atomic element

The Nuclear Magnetic Resonance (NMR) technique is applicable for the single atomic elements and for chemical compounds. In NMR technique the atoms are in a very strong homogeneous permanent (DC) magnetic field. An RF radiation is applied at a perpendicular (axis) or at angle to this field and the signal is taken by a sensitive magnetic detector aligned at another axis, which is perpendicular to the DC and RF axes. The RF field causes the individual atom to rotate, but then it interacts with the strong magnetic field. In result of this interaction, the whole atomic structure obtains oscillation motion with a precessional component due to the interaction of its close proximity fields (possessing a helical feature) with the external fields.

It is obvious, that the orbital planes should play an important role in the precessional motion. This means, that the electrons participate in the complex motion by transitions between the energy levels. The contribution of the external valence protons, with its orbiting electrons should be stronger as the relative electron speed of these electrons referenced to the nuclear electrons (referenced also to a local rest frame) is larger. By detecting the signature of the precessional motion a spectrum is obtained, known as a NMR spectrum. When a more precise scanning is performed, the signature of the electron transitions appears. This technique is known also as an Electron Paramagnetic Resonance (EPR).

The NMR can be applied for elements and for the molecules (chemical compounds). When applied for elements, one specific feature deserves to

be mentioned. **The detection efficiency is optimal, when the RF field is applied at 54.4^0 to the strong magnetic field (instead of at 90 deg). This effect could appear only if the atoms possess a helicity.**

The angle of 54.4^0 is not a twisting angle, of the atomic structure. It provides only an indication about the higher order helicity of the atom.

8.8. Giant resonance

Presently heavy atoms mostly are used for experiments related with the nuclear giant resonance. The BSM explanation of this effect is quite straightforward. The effect is caused by the vibrational motion of the neutron around the proton saddle. Therefore, following the Z-trend of the Periodic Table, the Giant resonance will become apparent from the Deuteron and its signature will become more complex with the increase of the Z-number. The intensity of this type of resonance is quite high because the large neutron mass is involved. The resonance peaks in the heavier atoms are contributed by the separate groups of the Deuterons and Tritium.

8.9 Scattering experiments

The shape of the atomic nucleus according to the QM model is close to the sphere with dimensions much smaller, than the electron orbits. This assumption came initially from the interpretation of the Rutherford's experiment, provided in 1906. In this experiment α particles (He nucleus) from radioactive source strike one or pair of golden foils at normal incidence. The angles of their deviation from the initial direction are measured by large photographic plate behind the foils. Most of the alpha particles passed clear through, unaffected and undiverted, recording themselves on the photographic plate behind. There were, however, some particles that were scattered even through large angles. Since the gold foil was about two thousand atoms thick, and since most alpha particles passed were not deviated, it would seem that the atoms were mostly empty space. Since some alpha particles were deflected sharply it has been interpreted that somewhere in the atom must be a massive, positively charged region, capable of turning back the positively charged alpha particles. Rutherford

concluded, that the atomic nucleus is very small but containing all mass and the total positive charge. He admitted that the atom has a planetary model with a mass concentrated in the small spherical nucleus, while the electron circles around the nucleus as planets. In the contemporary physics this concept has not been changed too much since the time of the Rutherford's experiment.

The data analysis the Rutherford's experiments is based on the following considerations:

A. Considerations: The following assumptions are adopted:

- the nucleus has a simple spherical structure and its positive charges are located in extremely small volume inside the sphere. (later the charges are considered distributed in the nuclear volume);
- the alpha particle does not have a structure;
- the inertial mass and the Coulomb force (according to inverse square law) are valid at small distances (below the Bohr radius)

Applying these considerations the Rutherford experiment leads to a nuclear size in order of $1E-15$ m.

According to the BSM for the correct interpretation of the data from the same experiment, the following considerations, should be used:

B. BSM considerations: The following features must be taken into account:

- inside the golden foil the CL space is not uniform but spatially modulated by the hadrons building the atomic nuclei
- the shape factor of the atom of Au and the distributed E-field inside the Bohr surfaces of the protons
- the crystal structure formed by the Au atoms
- the shape factor of the He nucleus and its helicity
- the complex structure of the proximity E-fields around the individual atoms

Using the real atomic models of BSM, it is evident that the interaction mechanism is much more complicated and any simple model for data interpretation is not adequate. The channel structure of the Au crystal is also one major factor. For these reasons the data interpretation according to **considerations A.** may lead to a quite different atomic model than the real one.

The data interpretation of the Rutherford's experiment according to BSM theory is quite different. Fig. 8.22 helps to provide some qualitative insight about the interactions between He nuclei and the golden foil. The drawing shows only one layer of the crystal lattice structure of Au, corresponding to the left panel of Fig. 8.17 (T. Kawasaki et al. (2000)).

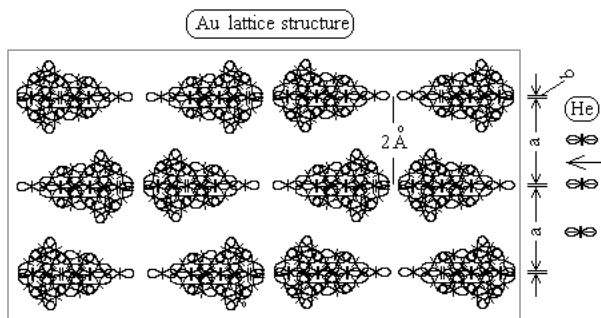


Fig. 8.22 Illustration of the scattering experiment (Au thin foil irradiated by α particles)

The dimensions of He and Au nuclei are given in one and a same scale. The width of the "pass through" zone is annotated by a , while the deflected zone by b . Due to the helical interactions be-

tween the alpha particles and atomic nucleus (by their fields), the atomic crystal provides a guiding of the alpha particles, that makes $b \ll a$. For this reason a small amount of alpha particles are deflected. The channelling structure of the metal crystal will affect tremendously the propagation of the particles in such type of scattering experiments.

8.10 Three dimensional view of the atomic nucleus

Providing an accurate three dimensional view of any atomic nucleus is not so simple, due to the nuclear helicity. Fig. 8.23 and 8.24 show two views of a mechanical mock-up made by steel springs. The upper part of the structure in Fig. 8.23 corresponds to Ar atom (only four neutrons over equatorial GBclp are missing). The lower part is a modified He structure with EB bonds. The same figure shows, also how the lower structure is clamped to the upper Ar-like structure by GBpc bonds. If one additional Deuteron is bonded in the bottom of the whole structure, the shape of Cu atom will be obtained.

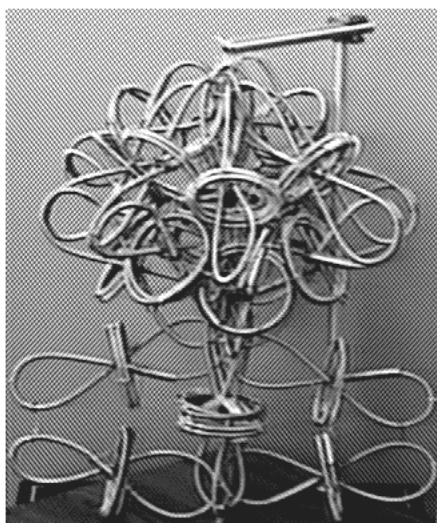


Fig. 8.23

Front view of mechanical mock-up

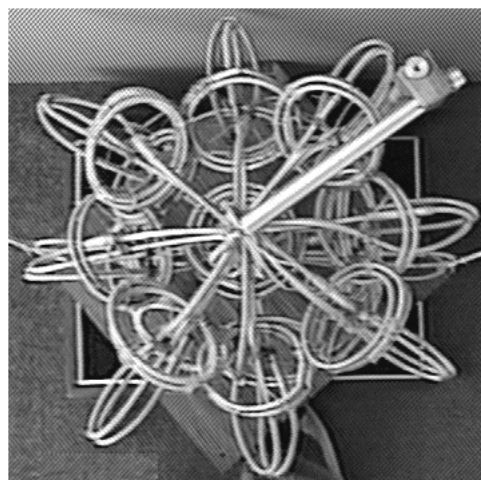


Fig. 8.24

Polar view of mechanical mock-up

8.11 Electron series in the atoms at larger Z number

The electron orbitals of Hydrogen atom ap-

pear in a similar way in other atoms, with exception of the Helium. The two electron orbitals of the Helium lie in two well separated planes parallel to the equatorial plane of the nucleus. They may interact

magnetically (by the QM spin), but any transition between them are not possible.

The appearance of the Hydrogen-like orbitals in all other atoms exhibits some restriction in result of nuclear configuration. Balmer series is one of the most important series. It appears in the free end club of any valence proton (not involved in a chemical bond). The orbital quasiplane of the Lyman series, however, has to pass through the polar region. So this series is less restricted, when the element is in a vapour aggregate state of the matter, than in a solid state.

While the orbitals in heavier atoms are subordinated on the same quantum orbital rules as in the hydrogen (and deuteron), their energy levels are modified due to the following additional conditions:

- **The Ground State (G.S.) appears shifted and the series range spanned in a result of redistribution of the intrinsic gravitational and electrical field inside the integrated Bohr surface.**
- **The orbital interactions between different protons change the conditions for the electron transitions**

8.12 Spin orbit interaction

For the Hydrogen atom, the G.S. of all series is one and same. The valence electron behaviour of the I-st group alkali atoms is the same. The ions, that have lost all the electrons but one, have also the same type of Hydrogen like spectra (only different energy levels). It is evident, that the electron transition behaviour for all atoms having only one electron in their external shell is similar. In other words, the levels are not split. This means, that the electron from the G.S. for example jumps to upper orbit, when a photon is absorbed, and after the elapsing of the quantum orbit time, falls back to the G.S. Let us use the terms “**excited**” and “**de-excited**” for characterization of the electron behaviour in the both states.

The individual electron behaviour in a neutral atom with more than one electron in its external shell is not identical to the electron behaviour in the hydrogen. Let consider the electron behaviour in Be atom for the case of spontaneous emission. The configuration of the Be atom with the two valence

protons and their electron orbits is illustrated in Fig. 8.25.

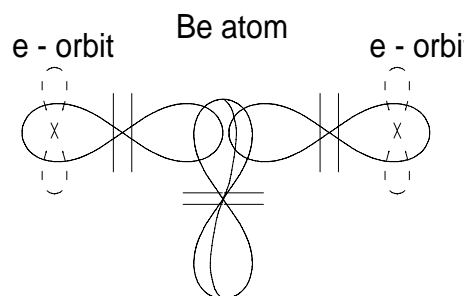


Fig. 8.25

Spin orbit interaction in Be atom. The planes of the two electron's orbits shown by dashed line are in fact normal to the drawing.

The size of the quantum orbits shown in Fig. 8.25 corresponds to the Balmer type series (but the energy levels are distinguishable from the Balmer series level of Hydrogen, because the CL space surrounding the nucleus is shrunk). Let assuming the two electrons have been in Balmer G.S. orbit for a time long enough, that their QM spins are parallel (matched). In some moment the first electron, for example, is excited and jump to some upper orbit above the Balmer G.S.. After its orbital time it elapsed, it must return to the Balmer G.S. orbit. This process could not be momentary. It should take a finite time, nevertheless, that it may be smaller, than the orbital time. The electron has to pass through a new region of the CL space, not procured like the orbital trace, where it also exhibits different IG forces and inertial mass. The latter parameter is affected by the different value of λ_{SPM} , whereas the CL node distance is the same (neglecting the general relativistic CL space shrinkage, that is negligible). The former orbital trace contains CL space energy pumped by the electron quantum motion in a closed loop. This energy could not be contained any more in this space and has to be emitted (as a quantum wave). The pumped energy, however, has to overcome the Bohr surface barrier. The reaction effect of this barrier, causes, some energy to be reflected back. It is reasonable to consider, that the Bohr surfaces of the paired protons are integrated. In such case, the reflected back energy could be temporally received by the second electron due to magnetic field interaction. Let suppose, that this energy is smaller in order to excite the sec-

ond electron to higher orbit. However, it may be enough to switch its QM spin in anti parallel state. This change will influence automatically the E-filed distribution of the first proton. In result of this, the quantum condition of the GS orbit will be satisfied for distance from the proton core different, than the initial one (estimated in absolute units of CL node distance). The gradient of the IG field near the proton core is highly dependent of the distance, so small distance change in absolute units means a large potential shift. As result, the GS level appears shifted. It is possible the next electron excitation to start from this shifted GS level. This shift in fact appears symmetrical for the second electron as well. The next excitation for one of both electrons may start from this shifted GS level.

Two additional options exist between the QM spin of every electron and the proton handedness. Their handedness may match or mismatch. Then four combinations are possible. They define four different GS levels. This is in agreement with the spectroscopic observations. Indeed if we examine the Grotrian diagram for a neutral Be atom, we see, that the lower energy state corresponding to a quantum number 2 has four levels: $2(0)$ for ns^1S ; $2(1)$ for np^1P^o ; $2(0)$ for np^1S and $2(2)$ for np^1D .

The above described process is a QM spin-orbit interaction in the atoms. One must keep in mind that this is a quantum mechanical spin, attributed to the orbital motion of the electron. It should not be confused with the electron spin momentum described in BSM as a classical feature of the rotating electron.

For atoms possessing larger number of external shell protons, the QM spin-orbit interactions could provide large number of level splitting and level shifts. Large shifts are possible especially for the elements from group 14 to 17, because the EB bonded external protons may combine positively their QM spins.

8.13 Identification of orbits according to QM notation

The calculations of the atomic and molecular spectra by the Quantum mechanical methods are based on the electron configuration. They are separated in shells and subshells. Without going into details, we will show that the orbital planes in

the BSM models have definite features to be attributed to the the classification of QM model. The BSM models however are quite more informative about the spatial configuration of all electronic orbits and their freedom. Now the BSM models do not have a developed mathematical technique for a spectral calculations as the QM model, but this is not their purpose. Their advantages are in the possibility to obtain the configuration and mutual positions of the orbital planes. At the same time they possess the same energetic levels not only about the excited electrons but also the same ionization potentials (as the QM models).

Figure 8.25.A shows the graphs of the experimentally determined ionization energies of the first 21 elements of the periodic table.

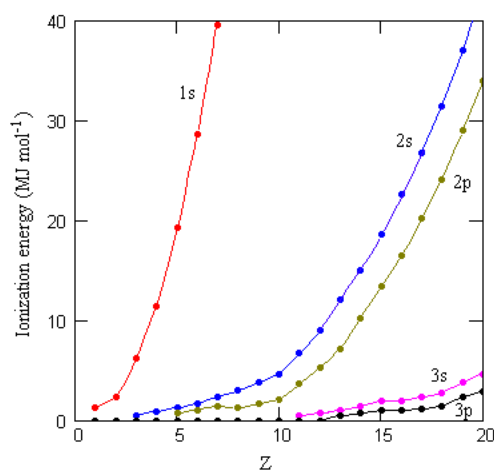


Fig. 8.25.A

Ionization energies of the first 21 elements

The trend between the different states denoted as 1s, 2s, 2p, 3s, 3p are quite apparent. But this trends clearly shows some features of the BSM model. They are the following:

The QM orbits denoted as **1s orbits** correspond to the polar orbitals. The orbital planes are perpendicular to the polar axis (the cosines of their normals in respect to the polar axis are equal to 1). They are located in high gradient IG fields. Their quantum levels are strong and grow faster with Z number, because every new added proton increases the polar IG field. For this reason their QM interaction are also strong and they always have an opposite QM spins. For this reason the quantum level of these two orbitals are exactly the same.

2s and 2p orbits from ${}^3\text{Li}$ to ${}^9\text{F}$: corresponds to the **Balmer type orbits connected to the free club of the valence protons (see Balmer series model in Chapter 7)**. Having in mind that the potentials are estimated by a photoelectron spectral technique, it is apparent why the trend of 2s is above the trend of 2p. It is a result of the Hund's rule orbital pairing. The electron of unpaired orbit is removed easier, than the paired one.

2s and 2p orbits from ${}^{10}\text{Ne}$ to ${}^{18}\text{Ar}$: correspond to orbits of the equatorial GBclp bonded protons (deuterons). Every orbit contains two electrons with opposite QM spins around two proximity connected proton clubs. For this reason, their quantum energy grows much faster. The spin orbital interaction between this orbits is also much larger, due to their well fixed positions and symmetry in respect to the polar axis. The larger QM spin interactions also contribute to the difference between 2s and 2p trends. This is in agreement with the considerations about the strong line pairing in characteristic spectral lines in X spectral range discussed in §8.4.4.2

3s and 3p orbits from ${}^{11}\text{Na}$ to ${}^{17}\text{Cl}$: correspond to Balmer type of orbits connected to the free proton clubs. They are much more peripheral and their removal is easier. Even EB bonds (Hund's rule pairing) are not so strong, so the difference between 3p and 3s is much smaller.

Figure 8.25 shows mostly the bottom range of the Ionization energy in order to emphasize on some features. We may see (a good plotting accuracy is needed) that 2 and 3 (s and p) trends are not very smooth at some Z numbers.

There is a change of the 2s and especially the 2p trend for $Z = 7$. This corresponds to oxygen that obtains two symmetrical GBclp in the equatorial region. The planes of corresponding orbits have cosines in respect to the polar axis approaching 1, as in the case of the 1s orbits. The QM spin interactions in such condition are quite strong. Their ionization energy corresponds to the state 2s. When one electron is removed, the common symmetry is significantly deteriorated and the ionization energy is much lower. This may explain the ionization energy drop of the 2s trend.

There is a slop change of 2s and 2p trend between ${}^{10}\text{Ne}$ and ${}^{11}\text{Na}$. At Ne, all protons from the previous external shell becomes GBclp bonded

in the equatorial region. The number of these protons is an even number and the normals of the corresponding orbital planes obtain a cosine close to unity. All the electronic orbits of Ar are well aligned, so they may obtain a common QM spin that could be right or left handed in respect to the proton handedness. **For this reason the QM spin has a strong feature apparent in the electronic spectra of argon.** In ${}^{11}\text{Na}$ a new proton shell is started. The 2s and 2p states for Na lie little bit above the common trend. In such case a possible equatorial shrink of the proximity CL space for the two diametrically situated protons is not excluded (this issue may need a special discussion).

The trend of 3s and 3p shows a slight change at ${}^{18}\text{Ar}$. For this atom all 16 protons (deuterons) from the external shell are equatorially bonded in 8 GBclp type bonds. The difference in the trend is not large because ${}^{40}\text{Ar}$ has four external neutrons over the four GBclp, while other four GBclp does not have such neutrons. The neutron over GBclp eases the electron removal and this contributes to the smoothness of the trend.

Another apparent change of trends 3s and 3p is between ${}^{15}\text{P}$ and ${}^{16}\text{S}$. This is caused by the GBclp of two proton pairs in the equatorial region in S. In fact the effect is similar as the described above effect at oxygen atom.

Despite the significant change in the nuclear configuration we see, that the trends of 2s, 2p, 3s, 3p and so on look pretty smooth. This may lead to the following conclusions:

- **the Bohr surfaces of the internal proton shells are well integrated**

- **the smoothness of the ionization energy curves indicates that the IG field is able to redistribute the E-field in the integrated Bohr surfaces to some extent, so the positive charge in the far field looks like a point charge**

The above made conclusions are additionally confirmed in the course of BSM.

Discussion: The QM model of electronic configuration of the atoms provides information mainly about the common orbital plane directions. The BSM model provides the full physical picture of the orbital planes and their common positions. It is evident that the orbital shells and subshells identified from QM model do not coincide with the physical shells of the proton arrangement and con-

nected to them orbits according to BSM models. This discrepancies increases with the increase of the Z number of the element.

It is worth to mention that despite the mentioned discrepancies both, the QM and BSM models exhibit the following common features:

- The protons arrangement in shells matches exactly the periodic table of the elements

The BSM model additionally contributes one useful feature, that is not apparent in the QM models.

- The orbital plane positions, which are the most important factors for QM spin interactions, are defined by the proton configurations in the nucleus

8.14 Ions

The ions are atoms, that have lost or accepted electrons. In the first case, the atom is converted to a positive ion, while in the second case - in a negative one.

In neutrals, the electrical fields of the system of protons - electrons are compensated inside the Bohr surface, so outside of it the atoms appears neutral, despite the different structures of protons and electrons. The neutralization effect is a result of dynamical interaction between the proton static field and the electron's dynamic field. In such case in the absent of disturbing external field we may consider that the both - the electrical and the magnetic field of the system are locked inside the Bohr surface. The conclusion made for a system of one proton and electron (H atom) should be propagated for a system of equal number of protons and electrons (any stable atom). Then the concept of Bohr surface defined for Hydrogen could be applied for any neutral atom. Having in mind the proton clubs proximity in the polar bonding region, it is logical to accept that the individual Bohr surface of the protons for atomic nuclei with $Z > 1$ are integrated in a **common Bohr surface**. This conclusion is in agreement with the concept of the charge appearance in the positive ions, discussed in the next paragraph.

8.14.1 Positive ion

The lost electron might be from a valence proton (external shell proton) or from the internal

shell. In the second case, known as Auger effect, the missing in the internal shell electron is replaced by some electron from the valence shell. So we may consider only the case of ions, obtained by losing of valence electrons. From the experimental investigation of the structure of ionic crystals (for example NaCl) and from the anion and cation components in the electrolytic solution it appears in first gland that the charged ion behaves as a point charge. But in the same time we see that elements possessing a valence shell do not have completely symmetrical nuclei. Then a question arises: how the positive ion, for example, does appear as a point like charged particle? The physical explanation of this effect is possible if admitting that:

(A) The Bohr surface of the atom is integrated from the individual Bohr surfaces of the protons involved in the nucleus.

According to conclusion (A) the common Bohr surface will sense the missing charge. Inside the integrated Bohr surface some E-filed gradient may exist, due to which any missing Auger electron is replaced by some valence electron. But even one missing electron from the external (valence) shell is able to disturb the integrated Bohr surface. In result of this a leak of E-field could emerge trough it. At some finite range from the nuclear centre, the electrical lines get a spatial rearrangement, so the positive ion appears as a point like charge in the far field. The accepted concept leads to the following conclusion:

(B) It is not possible to estimate correctly the atomic nuclear radius from the ionic type of bond.

A positive ion of Na is illustrated in Fig. 8.26.

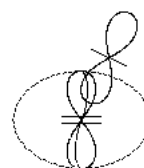


Fig. 8.26

Na⁺ ion illustrated by a polar section. The Ne nuclear structure is shown as oval.

8.14.2 Stable negative ions

Some elements may have stable negative ions, while others do not. The halogens, for exam-

ple have stable negative ions. They may participate in ionic molecular bonds. Other elements, like oxygen, for example, may form a metastable negative ion.

The explanation of the stability of the negative ion is not so simple as the positive one. Why the negative ion for some elements is stable, despite the disturbance of the atomic neutrality? The stable existence of the negative ion perhaps involves some mechanism opposing the disturbance of the integrated Bohr surface and assuring a suitable orbit of the accepted electron.

Let consider a negative ion of Cl, as a typical representative of halogens. It is not difficult to guess, that the accepted electron will share the orbit of the valence electron, but the partial freedom of the proton may allow it to obtain position similar as the EB bonded protons. This case is different from the EB bond in a neutral atom where the common orbit is shared by two electrons. In the latter case the position of the orbit is kept by two protons. In the case of negative ion (Cl^-) the valence proton, whose orbit is shared has some angular freedom in the polar plane. It is reasonable to consider, that both electrons occupy the Balmer orbital quasi-plane. The two electrons will not only neutralise (dynamically) the positive EQ's around the free proton club, but will create negative EQ's in a close proximity range. Then the free proton club may approach the equatorial region. **In this position the shared orbit may be oriented in a same way as the other orbits of the equatorial EB bonds.** (Notice, that the pairing for Halogens is by EB bonds). Then the electron configuration of the external shell may obtain more completed symmetry with the involvement of the accepted electron. This means, that **the position of the shared orbit of the valence proton might be kept fixed by the common magnetic field from all orbits inside the integrated Bohr surface.** This provides stability of the negative ion. This is kind of quantum mechanical orbital interaction.

- **The stability of the negative ion of the halogens, may be a result of the quantum mechanical orbital interactions inside the integrated Bohr surface.**

The possible configuration of the chlorine negative ion is shown in Fig. 8.27.

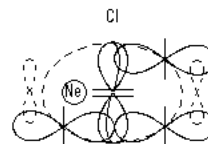


Fig. 8.27

A possible configuration of Cl^- ion illustrated by a single polar section. The Ne nuclear structure, which is embedded in Cl atom is shown as oval. The quantum orbit in the left side is magnetically infinite to other 3 EB orbits in the equatorial region of the nucleus

8.14.3 Size of the positive and negative ions.

According to the BSM concept the real nuclear size size of the ions does not corresponds to the size of the ions determined by the extension of the charge. This is evident from the comparison between Na^+ and Cl^- ions. The nuclear structure of Na^+ appears larger than the nuclear structure of Cl^- . In the existing so far data about the ionic radii, however, the radii of negative ions are given larger. The obtain discrepancy may have the following explanation:

(1) The ionic radius measured experimentally is a signature of the integrated Bohr surface rather than the nuclear structure. In the ions, the integrated Bohr surface is disturbed, when compared to the neutral atoms. This means that the leaked E-filed lines in ions are rearranged until obtaining some equivalent radius, which is always larger than the nuclear structure.

(2) The larger size of the negative ions could be also a result of asymmetry between the negative and positive prisms that propagates in the CL space.

From the provided concept, it follows that the nuclear radius could not be estimated from the ionic radius.

8.15 Some aspects of photon emission and absorption

The physical aspects of the quantum wave has been discussed in Chapter 2. The mechanism of photon emission and absorption presented by the Balmer model in Chapter 7 is valid for the other atoms but with additional considerations about the

IG field influence and the spin-orbit interactions discussed in §8.10.

The most accessible orbits for emission and absorption are those corresponding to the Balmer series in Hydrogen, which are physically connected to the free clubs of the valence protons (deuterons). Due to the IG field, their quantum levels appear higher than in the Hydrogen. The quantum orbits around the equatorial EB and GBclp bonds also are able to emit or absorb photons. Finally the two polar electrons (*s* electrons according to QM) also could generate photons at much shorter wavelength range, due to the large concentration of IG fields in the polar region. But all of this quantum orbits are not able to generate quantum waves (photons) in the X range of the spectrum. Such quantum waves are possible to be generated by the electron-positron oscillations of the orbiting electrons.

One specific feature of the quantum orbits connected with the valence protons is their possibility to be polarized. This means, that they may absorb a polarized photon and emit a polarized one. This is especially valid for the transition between the Balmer GS and the upper quantum level.

One example of such emission is the resonance scattering of Na at 689 nm. If the transition is activated by a laser source with a strong polarization, the emitted photon appear also polarized. The polarized photon exhibits E vector modulated strongly in one direction. This feature is valid for the whole length of the photon's wavepacket. It is quite reasonable to expect that the plane of the orbit activated by a polarized laser source is tilted from its normal position. This is illustrated by Fig. 8.28..

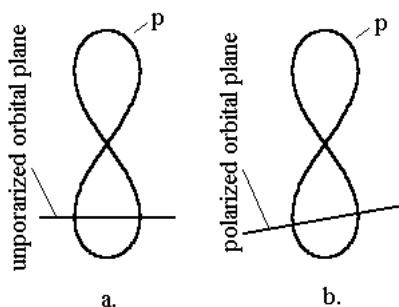


Fig. 8.28

Free valence proton with unpolarized (a) and polarized (b) orbit involved in resonance scattering process

The process of resonance scattering helps to unveil the physical mechanism of the photon emission and absorption. Let analyse only the absorption mechanism for the example with Na scattering at 689 nm. The tilting of the orbit points out to two features of the process:

(a) the energy distributed in the wavetrain with transverse diameter of about 689 nm shrinks about 20000 - 30000 times in order to dissipate in the range of magnetic radius swapping the orbit trace.

(b) the process of energy shrink is quite fast; perhaps the IG field interaction process is directly involved

(c) the energy shrink process may be regarded as wavetrain winding: but with a preservation of the spatial position of the polarization

(d) the alignment of the wavetrain shrinkage and the long axis of the valence proton is apparent

(e) in the final moment of the shrunk wavetrain the atomic nucleus may play a role of a reflector

The feature (b) indicates, that the process of wavetrain shrinkage could not be regarded as a simple winding, but more complicated processes related with the quantum quasishrink effect. This effect appears as static in the case of atomic spectra. It appears as dynamic in the case of molecular spectra and it is discussed in Chapter 9.

The above features could give a bare picture how the absorbed polarised radiation (mainly by laser source) could cause a tilt of the orbital plane.

8.16 Ferromagnetic hypothesis

Iron is one of the very abundant elements in the meteorites. The main reason for this is that the nuclear reactions lead to this element from both sides: by nuclear syntheses and by nuclear depletion. In the same time iron is highly ferromagnetic, when in solid state. The ferromagnetism appears quite strong also for its neighbours in the periodic table Ni and Co. In a proper mixture of them the magnetic susceptibility even increases. The opposite effect of the ferromagnetism is the diamagnetism. A proper parameter characterizing the elements for both phenomena is the Magnetic susceptibility of the elements. The magnetic suscepti-

bility of the elements in function of the Z number (a well known data) is shown in Fig. 8.29.

Note: The magnetic susceptibility parameter is valid when the element is in a solid state..

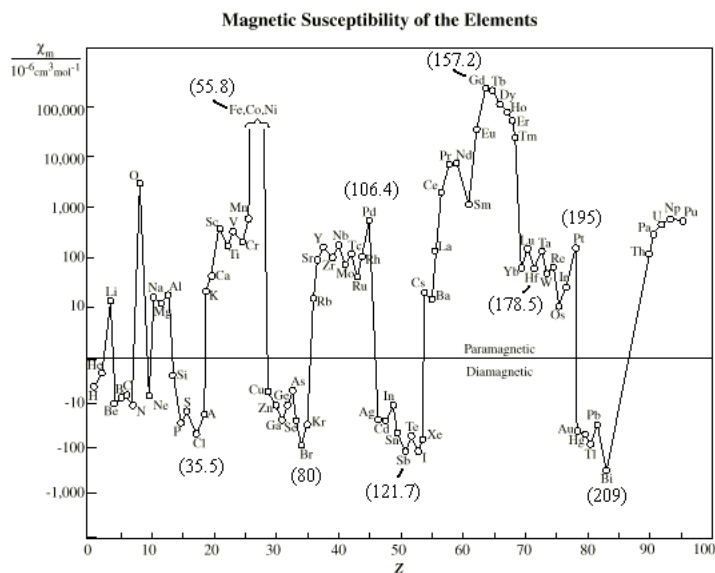


Fig. 8.29. Magnetic susceptibility of the elements

For ferromagnetic materials the magnetic susceptibility is a positive large number, while for diamagnetic it is a negative one.

Let analyse the trend of the magnetic susceptibility in function of Z number. It has the following important characteristics:

- (a) the trend of magnetic susceptibility exhibits periodical feature but with not a constant period
- (b) the positive peaks of the trend are much larger
- (c) the trend exhibits a steep change between some neighbouring elements of the periodic table

In Chapter 10 the concept of a local CL space around the FOHSs of the proton and neutron is discussed. Different elements have different nuclear binding energy, which is expressed by the mass deficiency. According to the BSM concept, even a single atom slightly modulates the surrounding CL space (GR effect in a proximity to the atomic nucleus). In the solid state of the matter one additional feature is added: the atoms are connected in a crystal. This factor is much stronger for the metals where the interatomic distances are smaller. For any macrobody in the Earth gravitational field for which the mass is much lower than the Earth

mass the Earth CL space (a modulation of the galactic CL space) penetrates inside the body. Consequently the solid body and especially a metal solid body could be able to modulate the penetrated CL space. The modulation of the CL space means a slight change of the mean CL node distance for some domains. So the CL nodes of these domains will obtain a different resonance and SPM frequency. It has been shown in Chapter 2, that one of the basic features of the magnetic field is the phase synchronization between the SPM frequency of the involved nodes which is propagated with the speed of light.

Consequently, the domain with a changed SPM frequency will affect the propagation of the magnetic field.

The change of the SPM frequency of such domain obviously should depend on the number of protons and neutrons in the atomic nuclei and the number of free proton clubs. These two parameters are changing simultaneously with the Z-number and contribute to a feature (a) of the trend.

It is obvious that the changed SPM frequency of the affected CL domains will be higher than this of the normal CL space. This is in agreement also with the refractive index change for metals measured by X rays. **Then for some Z-numbers the changed frequency of some particular domains**

may become a harmonic of the normal SPM frequency. In this case the magnetic susceptibility could obtain a large value.

The magnetic susceptibility may not arise only at exact harmonics. The magnetic quasisphere (MQ) of the SPM vector has 6 bumps and dimples between them. The NRM vector spends more time in the bumps, than in the dimples (this is a quantum feature of the CL space). This feature provides a possibility for synchronization between neighbouring domains with SPM phase difference not only of 2π , but also of $2\pi/6$. (factor 6 is the number of bumps). This of cause is related with a space-time parameter λ_{SPM} and requires finite length in space. So some stroboscopic effect may appear related to λ_{SPM} .

The above described features may explain the quasi periodical appearance of the magnetic susceptibility trend. The diamagnetism, however, (the negative value) requires some additional explanation. For this purpose Fig. 8.30 illustrates the 3D shape of the magnetic quasisphere (MQ) viewed from two opposite directions.

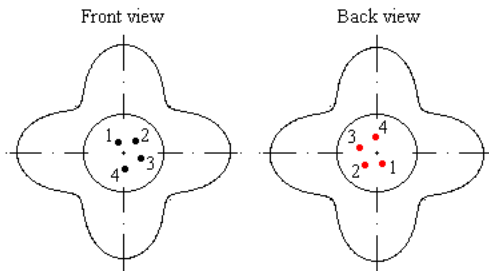


Fig. 8.30

Front and back view of consecutive positions of NRM vector. Positions in the front view are shown as black points, while in the the back view by red points.

The positions 1,2,3,4 are consecutive positions of NRM (node resonance momentum) vector on two opposite bumps of MQ. So the black and red points are time separated by half of resonance cycle. Every consecutive position is displaced from the previous in an order defined by the rotational direction of the NRM quasisphere. If referencing the position 1 as initial phase position of SPM vector it returns to it after N_{RQ} number of cycles of NRM vector. Then the SPM vector will pass through the

same point after a phase of 2π or $n2\pi$, where n is an integer. The rotational direction of NRM determines the two different option for SPM vector related with clockwise and counter clockwise circular polarization. In the front view of MQ, the rotational direction is clockwise, while in the back view it is a counter clockwise. In the real case, the points are very close because the surface of an equivalent sphere is obtained by $N_{RQ} = 0.8843 \times 10^9$ number of resonance cycle. So there is one important feature:

(A) $(2n-1)\pi$ **odd phase conditions of the SPM vector**: For a limited number of resonance cycles the direction of rotational motion may not be distinguishable due to some threshold noise. Then for a limited time the position of SPM vector could appear the same not only for a phase difference of $n2\pi$, but also for a $(2n-1)\pi$.

Let considering two cases:

Case (1): the effect (A) is ignored (due to some threshold noise) and the SPM phase synchronization is at 2π or $n2\pi$. In this case the magnetic susceptibility will exhibit a quasi periodical dependence but only with positive values. When the phase synchronization condition deteriorates for some elements, the magnetic susceptibility declines towards lower values.

Case (2): the condition (A) is valid.

For a limited time a phase synchronization at $(2n-1)\pi$ may occur for the SPM vectors of some neighbouring domains. For a longer time duration, however, this wrong synchronization could be recognized due to the Zero Point Waves. The wrong temporal synchronization will cause some energy fluctuations tending to remove the **odd phase conditions of the SPM vector** $(2n-1)\pi$. The time duration of such event evidently should be smaller than the time-space constant. The effective force opposing the external magnetic field in this case will be a repulsive one, i. e. the material will appear as diamagnetic.

Note: In case (1) the effective attractive force could be regarded as a result of “catch and hold” effect whose strength depends of the degree of SPM frequency change

In case (2) the effective repulsive force could be a result of “wrong temporally catch and hold” effect.

According to the described concept the magnetic susceptibility is directly related to the node resonance frequency of the magnetic domains. The atomic mass is one of the major factor influencing the node resonance frequency of these domains. Then some periodicity between the atomic mass and the peak value of the magnetic susceptibility should exist. In Fig. 8.29 the atomic masses for some of the elements staying in the peak regions are shown as approximate peak values. One may identify:

approximate positive peak values: 55.85, 106.4, 157.2, 195

approximate negative peak values: 35.5, 80, 121.7, 178.5, 209

The trend is pretty disturbed after Gd because of the different nuclear configuration. Although some approximate periodicity of about 50 atomic units is apparent. It may correspond to a phase change with 2π . It is also apparent that the phase of negative peak periodicity is shifted at about 25 atomic units. This is in agreement with the presented concept. The variation of the period estimated by the atomic mass might be influenced also by the atomic arrangement in the solids, which may contribute to differences in the specific gravity.

The ferromagnetic hypothesis is additionally discussed in the Chapter 10 and 12 in connections to the magnetic fields in the planets and stars.